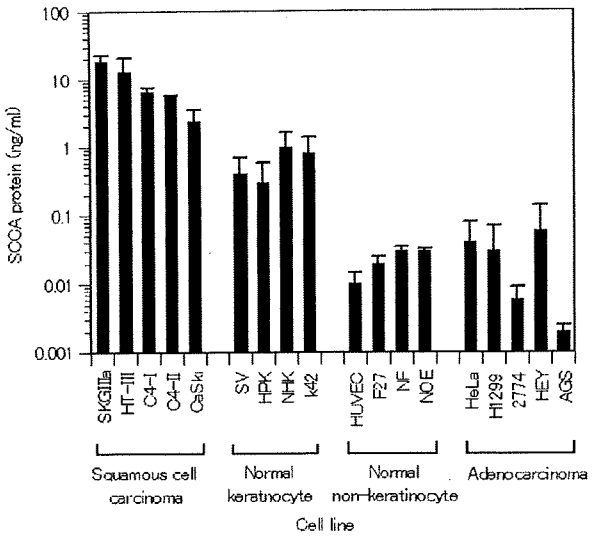

Figure 1. SCCA protein levels determined by ELISA in cervical squamous cell carcinoma, normal keratinocyte, normal non-keratinocyte and adenocarcinoma cells

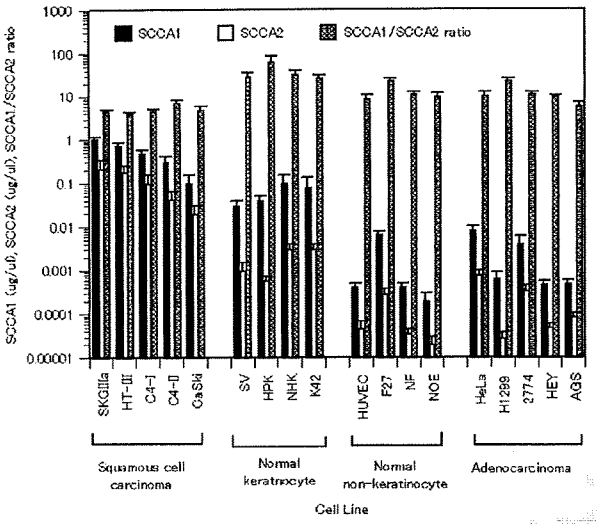

Figure 2. *SCCA1* and *SCCA2* mRNA levels determined by real time RT-PCR in cervical squamous cell carcinoma, normal keratinocyte, normal non-keratinocyte and adenocarcinoma cells

cells and 329-fold greater than that of adenocarcinoma cells. The mean level of SCCA protein secretion by keratinocyte cells was 28-fold greater than that of normal non-keratinocyte cells and 23-fold greater than that of adenocarcinoma cells. The mean level of SCCA protein secretion by normal non-keratinocyte cells was not significantly different from that of adenocarcinoma cells.

mRNA levels of *SCCA1* and *SCCA2* in cervical squamous cell carcinoma cells

To examine the mRNA levels of *SCCA1* and *SCCA2* in cervical squamous cell carcinoma cells, one-step real time RT-PCR was performed using MGB probe. The mRNA level of *SCCA1* was one or two orders of magnitude higher than that of *SCCA2* in all cell types examined (Figure 2). The mRNA level of *SCCA1* in cervical squamous cell carcinoma cells was 8.5-, 280- and 195-fold greater than that in normal keratinocytes, normal non-keratinocytes and adenocarcinoma cells, respectively. The mRNA level of *SCCA1* in normal keratinocyte cells was 33- and 23-fold greater than that in normal non-keratinocytes and adenocarcinoma cells, respectively. The mRNA level of *SCCA1* in normal non-keratinocyte cells was not significantly different from that in adenocarcinoma cells.

Transcriptional activities of *SCCA1* and *SCCA2* in squamous cell carcinoma cells

To examine the transcriptional activities of *SCCA1* in squamous cell carcinoma cells, transient expression assays were performed. Luciferase reporter plasmids containing varying lengths of the 5′-flanking regions of the gene were constructed (SCCA1-750, SCCA1-550, SCCA1-525, SCCA1-500, SCCA1-475, SCCA1-450, SCCA1-375, SCCA1-250, SCCA1-175, SCCA1-125 and SCCA1-75) as shown in Figure 3A and transfected into HT-III cells, and cell lysates were tested in luciferase assays. Figure 3B demonstrates the transcriptional activities in HT-III cells. Deletion analysis from the −750-bp to −525-bp region upstream from the gene revealed a gradual increase in transcriptional activity with a decrease in length, suggesting the presence of a sequence inhibiting transcriptional activities of the gene between −750-bp and −525-bp. A region from −525-bp to −475-bp of the *SCCA1* promoter demonstrated significant transcriptional activity. Deletion analysis from the −450-bp to −175-bp region upstream from the gene revealed a gradual increase in transcriptional activity with a decrease in length of promoter, suggesting the presence of a sequence inhibiting transcriptional activities of the gene between −450-bp and −250-bp. A −175-bp region of the *SCCA1* promoter demonstrated significant transcriptional activity. This proximal negative region from −525-bp to −475-bp and the positive −175-bp region have not been reported previously [8].

To determine the enhancer region, the intron 1 region or proximal promoter region from −525-bp to −475-bp was inserted upstream of the −175-bp region of *SCCA1* luciferase promoter plasmid. Luciferase reporter plasmids of SCCA1-175 containing intron 1 in sense or antisense orientation or the region from −525-bp to −475-bp were constructed (INT-SCCA1-175 for sense orientation of intron 1, INT-AS-SCCA1-175 for antisense orientation of intron 1, 525-SCCA1-175 for sense orientation of −525-bp to −475-bp, 525-AS-SCCA1-175 for antisense orientation of −525-bp to −475-bp, and 525-2-SCCA1-175, 525-3-SCCA1-175, 525-4-SCCA1-175, 525-5-SCCA1-175, 525-10-SCCA1-175 and 525-20-SCCA1-175 for tandem

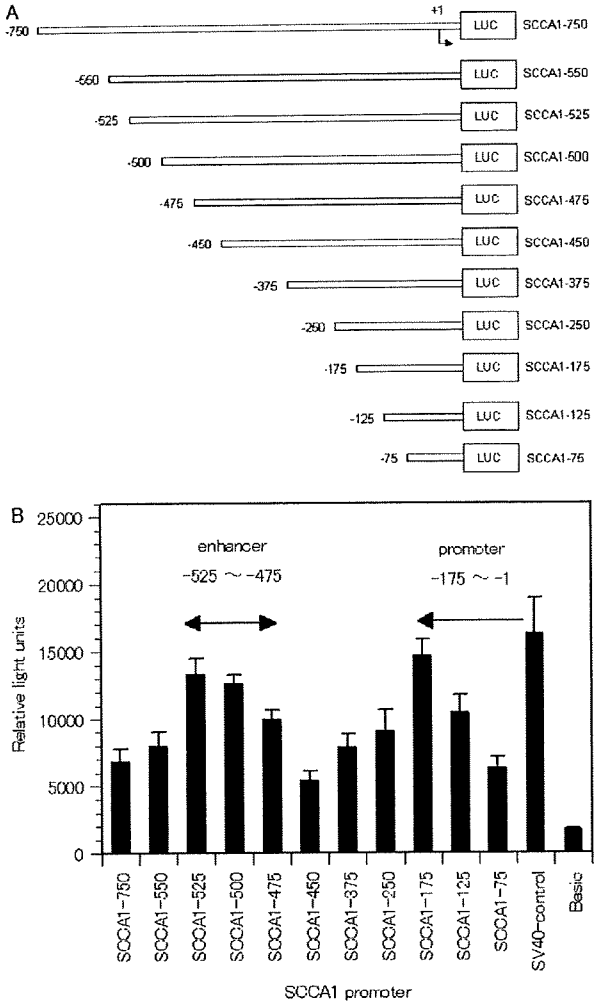

Figure 3. (A) A schematic representation of *SCCA1* reporter plasmids. 5′-truncated fragments of the promoter region upstream from the *SCCA1* gene were inserted into luciferase (LUC) reporter vector in sense orientation. Arrow indicates the transcription start site. Numbers indicate the number of bases upstream (−) or downstream (+) from the transcription start site. The name of each reporter construct was assigned according to the 5′-end nucleotide numbers of inserted promoter sequences, upstream of the transcription start site. (B) Transcriptional activity of *SCCA1* promoter in HT-III cell line, and identification of core promoter region. Bars indicate the SD

repeats of −525-bp to −475-bp) as shown in Figure 4A and transfected into HT-III cells, and cell lysates were tested in luciferase assays. Figure 4B demonstrates the transcriptional activities in HT-III cells. Intron 1 did not enhance SCCA1-175 promoter activity, consistent with a previous study [13]. However, the sense and antisense orientations of the −525-bp to −475-bp region significantly enhanced SCCA1-175 promoter activity, indicating that this region functioned as an enhancer for the SCCA1-175 promoter. Five tandem repeats of the −525-bp to −475-bp region increased SCCA1-175 promoter activity by up to four-fold, whereas ten or 20 tandem repeats of this enhancer region did not further increase SCCA1-175 promoter activity compared to five tandem repeats.

To compare the tissue specificity of the transcriptional activity of enhancer-promoter complex of *SCCA1* promoter, various numbers of tandem repeats of enhancer and SCCA1-175 promoters were transfected into HT-III squamous cell carcinoma cells and H1299 adenocarcinoma cells. The promoter activity of SCCA1-175 in HT-III cells was 20-fold greater than that in H1299 cells, and the promoter activity of five tandem repeats of the enhancer and SCCA1-175 in HT-III cells was 37-fold greater than that in H1299 cells (Figure 4C). Thus, five tandem repeats of enhancer and promoter complex exhibited significant tissue specificity in squamous cell carcinoma cells compared to adenocarcinoma cells.

To compare the tissue specificity of transcriptional activity of the enhancer-promoter complex of *SCCA1* promoter, SCCA1-175 with five tandem repeats of enhancer and SCCA1-175 promoter were transfected into squamous cell carcinoma cells, normal keratinocytes, normal non-keratinocyte cells and adenocarcinoma cells. The promoter activity of SCCA1-175 in squamous cell carcinoma cells was 2.4-fold greater than that in keratinocyte cells, 7.6-fold greater than that in normal non-keratinocyte cells and 13-fold greater than that in adenocarcinoma cells (Figure 4D). The promoter activity of SCCA1-175 in normal keratinocytes was three-fold greater than that in non-keratinocyte cells and five-fold greater than that in adenocarcinoma cells. The promoter activity of five tandem repeats of enhancer and SCCA1-175 in squamous cell carcinoma cells was five-fold greater than that in keratinocytes, 16-fold greater than that in non-keratinocyte cells and 30-fold greater than that in adenocarcinoma cells. The promoter activity of five tandem repeats of enhancer and SCCA1-175 in keratinocytes was three-fold greater than that in non-keratinocyte cells and six-fold greater than that in adenocarcinoma cells. The promoter activities of SCCA1-175 and SCCA1-175 with tandem repeats of enhancer did not differ significantly between normal non-keratinocyte cells and adenocarcinoma cells. Thus, five tandem repeats of enhancer significantly increased SCCA1-175 promoter activity in squamous cell carcinoma cells compared to normal keratinocytes, normal non-keratinocyte cells and adenocarcinoma cells.

Transcriptionally targeted AdE3-*SCCA1* has a potent antiproliferative effect in squamous cell carcinoma cells but not in normal non-keratinocyte cells or adenocarcinoma cells

To estimate the potential of *SCCA1* promoter for use in gene therapy for squamous cell carcinoma, *SCCA1* promoter-driven oncolytic adenovirus was constructed and transfected into each cell line. Figure 5A shows the construct of oncolytic adenovirus AdE3-*SCCA1* in which the 404–551-bp region of *E1A* promoter was substituted

by five tandem repeats of enhancer and SCCA1-175 promoter complex. Figure 5B shows the growth-inhibitory effects (IC_{50}) of oncolytic adenovirus AdE3-*SCCA1* in various types of cell lines. The IC_{50} of wild-type adenovirus AdE3 did not differ significantly among squamous cell carcinoma cells, normal keratinocytes, normal non-keratinocyte cells, nor adenocarcinoma cells. AdE3-*SCCA1* killed neither normal non-keratinocyte cells,

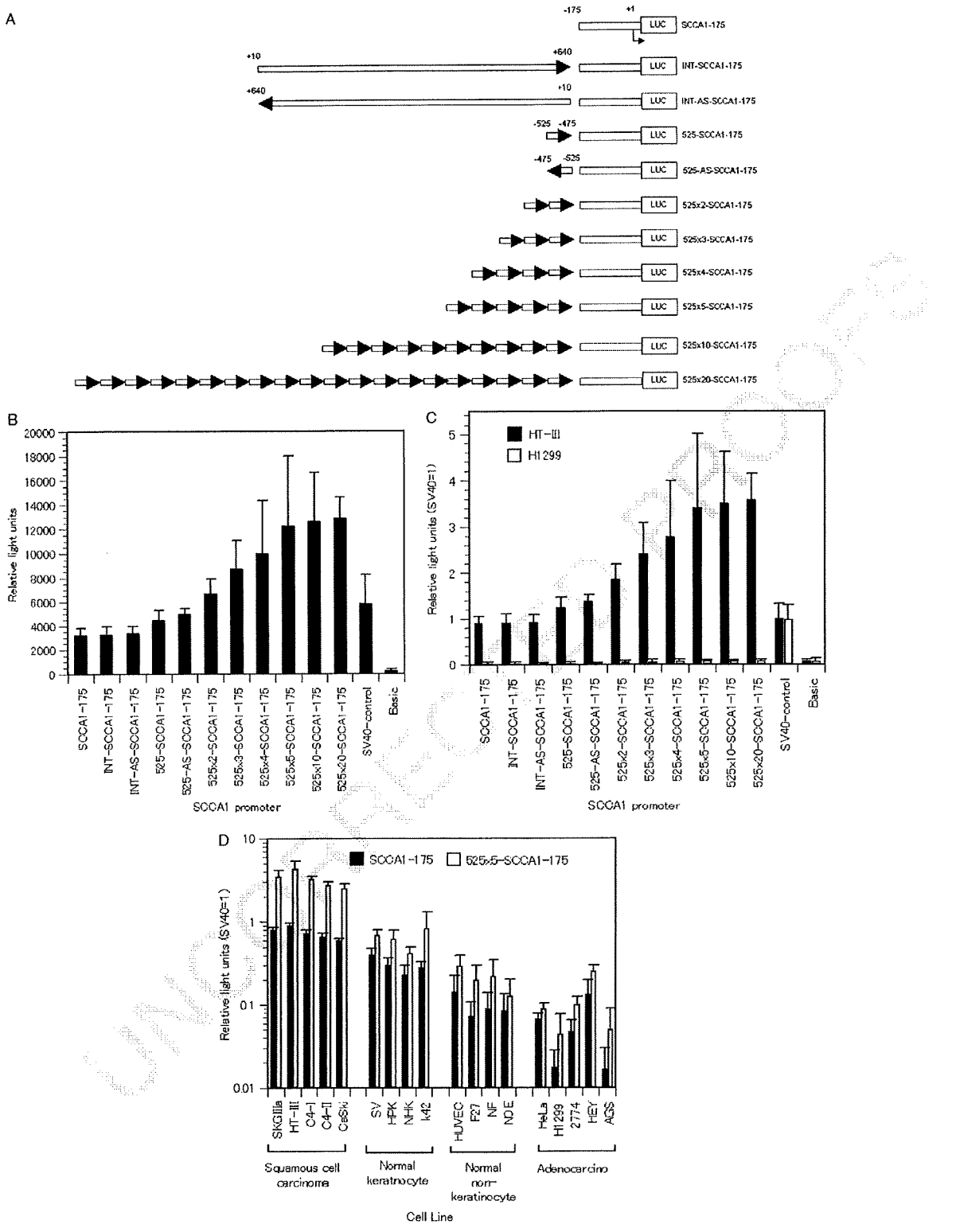

Figure 4.

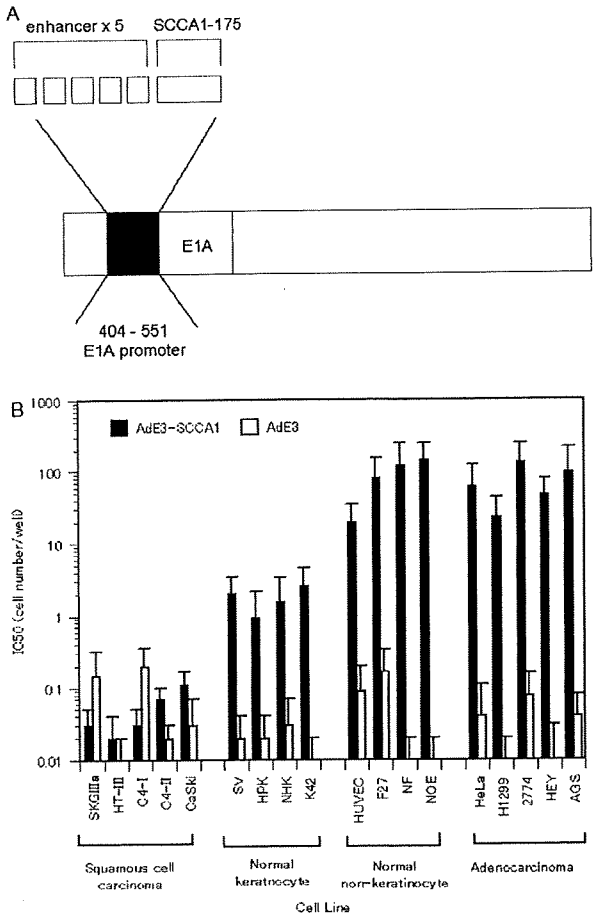

Figure 5. (A) A schematic representation of oncolytic adenovirus AdE3-*SCCA1*. SCCA1-175 with five tandem repeats from −525 to −475 bp was replaced with 404–551 bp of *E1A* promoter region. (B) The growth-inhibitory effects (IC_{50}) of oncolytic adenovirus AdE3-*SCCA1* and wild-type adenovirus AdE3 in cervical squamous cell carcinoma, normal keratinocyte, normal non-keratinocyte and adenocarcinoma cell lines. Bars indicate the SD

nor adenocarcinoma cells. AdE3-*SCCA1* significantly suppressed the growth of normal keratinocytes compared to normal non-keratinocyte cells and adenocarcinoma cells. Furthermore, this growth-inhibitory effect of AdE3-*SCCA1* was significantly enhanced in squamous cell carcinoma cells, and was one or two orders of magnitude higher than in normal keratinocytes.

Oncolytic adenovirus AdE3-*SCCA1* suppresses subcutaneous tumor growth of squamous cell carcinoma in nude and syngeneic mice

To evaluate the antitumor effects of AdE3-*SCCA1*, xenograftic subcutaneous tumors were established in the flanks of nude mice using cervical cancer HT-III and adenocarcinoma H1299 cells (Figure 6A). By 30 days, we observed a significant reduction in tumor size in the AdE3-*SCCA1*- and AdE3-treated groups compared to the medium alone- and Ad5CMV-*LacZ*-treated groups in the HT-III tumor models. AdE3-*SCCA1* and AdE3 significantly reduced tumor sizes by 95–98% compared to medium alone and Ad5CMV-*LacZ* ($p < 0.001$, unpaired *t*-test) (Figure 6B). By contrast, AdE3-*SCCA1* did not significantly reduce the sizes of H1299 tumors compared to Ad5CMV-*LacZ* (Figure 6C). However, AdE3 significantly reduced the size of H1299 tumors by 96% compared to Ad5CMV-*LacZ* ($p < 0.001$, unpaired *t*-test).

To evaluate the antitumor effects of AdE3-*SCCA1* after immunization, C3H mice were immunized with Ad5CMV-*LacZ* and subcutaneous tumors 5–8 mm in diameter were established in the left thigh of C3H mice using mouse squamous carcinoma SCC7 cells (Figure 7A). The survival of control mice was not significantly different from that of the mice treated with AdE3-*SCCA1* alone. We screened the 16 cell types of cells found to function as carrier cells for 293 and A549 cells [14]. Because A549 cells infected with oncolytic adenovirus were less damaged by freezing and thawing than 293 cells infected with oncolytic adenovirus, we used A549 cells as carrier cells. The A549 carrier cells all died within 2 weeks. The survival of mice treated with A549 carrier cells infected with AdE3-*SCCA1* was significantly longer than that of mice treated with medium control or AdE3-*SCCA1*. Furthermore, simultaneous infection with AxCA*mGM-CSF* augmented the antitumor effect of A549 carrier cells infected with AdE3-*SCCA1* ($p < 0.05$) (Figure 7B). Mice that exhibited complete tumor regression were resistant to subsequent inoculation of SCC7 cells.

Figure 4. (A) A schematic representation of *SCCA1* reporter plasmids with tandem repeats of enhancer region. The intron 1 region or proximal promoter region from −525-bp to −475-bp in sense or antisense orientation was inserted into upstream of the 175-bp region of *SCCA1* luciferase promoter plasmid. Tandem repeats of proximal promoter region from −525-bp to −475-bp were inserted into upstream of the 175-bp region of *SCCA1* luciferase promoter plasmid. (B) Luciferase activity of each reporter plasmid was examined in cervical squamous cell carcinoma HT-III. The plasmid (pGV-control) driven by SV40 enhancer/promoter was used as a positive control and pGV-Basic without enhancer/promoter as a negative control. Bars indicate the SD. (C) Luciferase activity of each reporter plasmid was examined in cervical squamous cell carcinoma HT-III and adenocarcinoma H1299 cells. The plasmid (pGV-control) driven by SV40 enhancer/promoter was used as a positive control and pGV-Basic without enhancer/promoter as a negative control. Luciferase activity in each plasmid was plotted as the ratio to the positive control plasmid (pGV-control). Bars indicate the SD. (D) Luciferase activities of reporter plasmids SCCA1-175 and SCCA1-175 inserted with five tandem repeats from −525 to −475 bp were examined in cervical squamous cell carcinoma, normal keratinocyte, normal non-keratinocyte and adenocarcinoma cells. The plasmid (pGV-control) driven by SV40 enhancer/promoter was used as a positive control and luciferase activity in each cell line was plotted as the ratio to the positive control plasmid. Bars indicate the SD

DOI: 10.1002/jgm

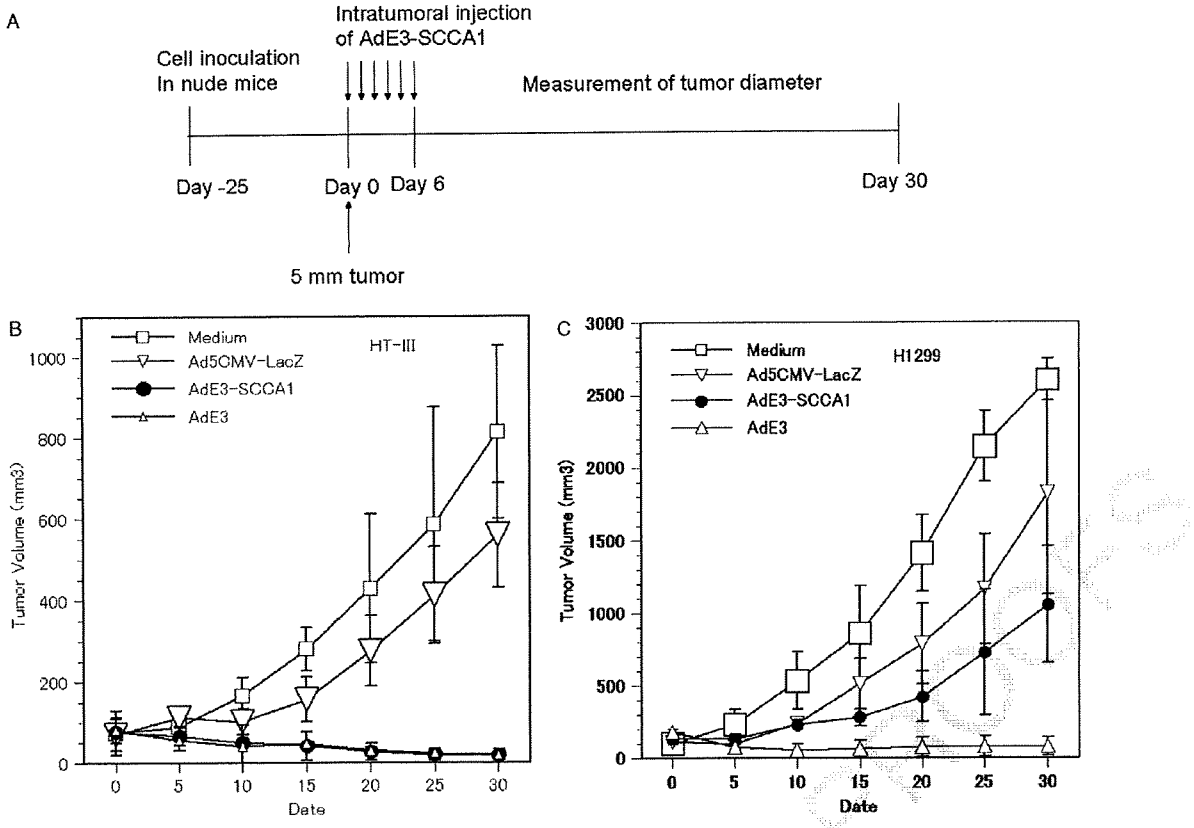

Figure 6. (A) A schematic representation of treatment schedule of oncolytic adenovirus AdE3-*SCCA1* in nude mice. (B) The antitumor effect of AdE3-*SCCA1* in subcutaneous cervical squamous cell carcinoma HT-III cell tumors in nude mice. (C) The antitumor effect of AdE3-*SCCA1* against subcutaneous adenocarcinoma H1299 cell tumors in nude mice

Discussion

In the present study, the highest *SCCA1* promoter activities were found in the 175-bp region just upstream of the *SCCA1* gene. It has been reported that a 0.5-kb fragment upstream of the *SCCA1* gene exhibited significant promoter activity [8]. This is consistent with the enhancer region and promoter activity identified in the present study. The negative element in the region 0.3- to 0.4-kb upstream of the *SCCA1* gene was reported previously [15], and corresponds to the negative 250- to 450-bp region in the present study. The positive 175-bp *SCCA1* promoter element had not been previously reported because the promoter activity of the 0- to 200-bp fragment of the *SCCA1* gene remained to be determined. The present study is thus the first to report promoter analysis of the proximal region of the *SCCA1* promoter and determine the maximal promoter activity of the 175-bp fragment of the *SCCA1* gene.

The present study also revealed an enhancer region 475-bp to 525-bp upstream of *SCCA1*. It has been reported that intron 1 in sense orientation alone increased 0.3-kb *SCCA1* promoter activity by two-fold, whereas that in antisense orientation did not increase it [15]. However, intron 1 in neither sense, nor antisense orientation increased *SCCA1* promoter activity in the present study, suggesting that intron 1 is not a major enhancer of *SCCA1*. Instead, we found that the 475-bp to 525-bp fragment increased SCCA1-175 promoter activity by 50% in sense and antisense orientations. The 475-bp to 525-bp fragment thus appears to be a major enhancer region of *SCCA1*. Double and triple enhancers further increased promoter activity compared to the single enhancer in the present study. Use of five tandem repeats of minimum enhancer element increased promoter activity the most, by four-fold, compared with one to four, ten or 20 tandem repeats of the enhancer element. Thus, five tandem repeats of minimum enhancer element significantly increased promoter activity and might enhance the amplification and the antitumor effects of replication-competent adenovirus.

SCCA protein, *SCCA1* mRNA, and *SCCA2* mRNA levels and SCCA1-175 promoter activity in squamous cell carcinoma cells were significantly higher than those in normal keratinocytes, which were in turn significantly higher than those in normal non-keratinocytes and adenocarcinoma cells. Although comparisons of *SCCA* gene expression and promoter activity among squamous cell carcinoma cells, normal keratinocytes and adenocarcinoma cells were reported previously [8,10], comparisons among squamous cell carcinoma cells, normal keratinocytes and normal non-keratinocyte cells had not previously

DOI: 10.1002/jgm

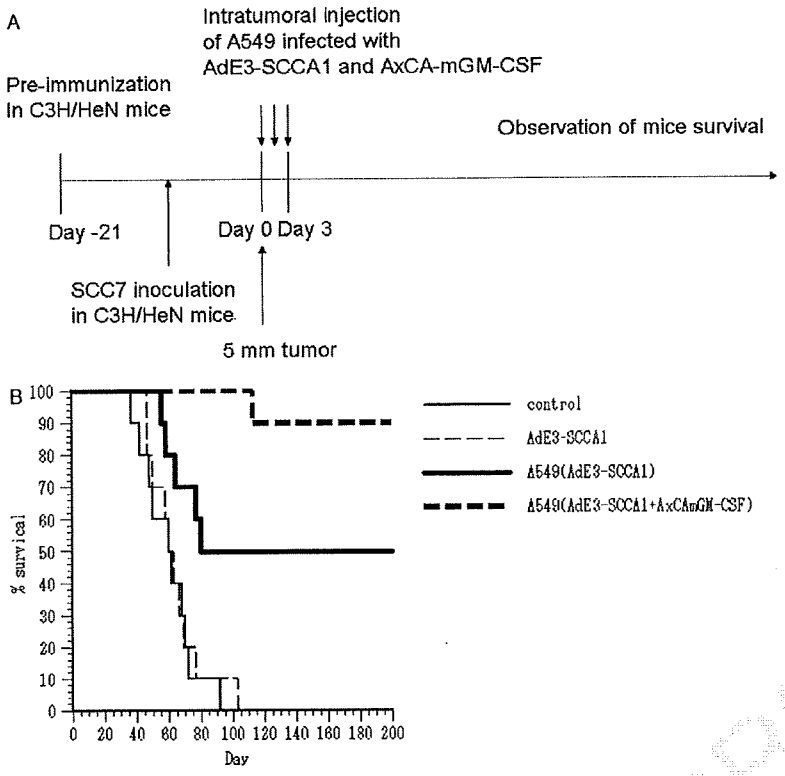

Figure 7. (A) A schematic representation of treatment schedule of carrier cells infected with oncolytic adenovirus AdE3-*SCCA1* and AxCA-*mGM-CSF* in syngeneic C3H/HeN mice. (B) The antitumor effects of AdE3-*SCCA1* against subcutaneous SCC7 tumors established in C3H mice after immunization. RPMI medium, AdE3-*SCCA1*, A549 carrier cells infected with AdE3-*SCCA1*, and A549 carrier cells infected with AdE3-*SCCA1* and AxCA*mGM-CSF* were injected into each tumor

been performed. SCCA1-175 and 525-5-SCCA1-175 promoter activities in normal keratinocytes were significantly higher than those in normal non-keratinocyte cells, and oncolytic adenovirus AdE3-*SCCA1* significantly suppressed the *in vitro* growth of normal keratinocyte cells compared to that of normal non-keratinocyte cells. These findings suggest that the *SCCA1* promoter might also be useful for gene therapy for skin diseases other than cancer.

The *SCCA1* to *SCCA2* mRNA ratio in squamous cell carcinoma cells was significantly lower than that in the other cells examined because the relative increase in *SCCA2* mRNA was significantly higher than that in *SCCA1* mRNA in squamous cell carcinoma cells compared to other cells. The adenovirus-mediated *SCCA2* promoter-driven proapoptotic gene thus induced selective tumor suppression of squamous cell carcinoma cells compared to adenocarcinoma cells [11], although this was not sufficient to induce complete tumor regression because *SCCA1* promoter activity is higher than *SCCA2* promoter activity in squamous cell carcinoma cells. We therefore used the *SCCA1* promoter for gene therapy for squamous cell carcinoma cells. Furthermore, although *SCCA1* promoter alone was not sufficient for overexpression of genes, five tandem repeats of enhancer increased *SCCA1* promoter activity by four-fold and increased the selectivity for squamous cell carcinoma by two-fold compared to that for the other cells examined.

The oncolytic adenovirus AdE3-*SCCA1* selectively killed squamous cell carcinoma cells *in vitro* and *in vivo*. Squamous cell carcinoma can occur in many different organs, including the skin, lips, mouth, oesophagus, urinary bladder, prostate, lungs, vagina and cervix, amongst others. Although oncolytic adenovirus vector driven by *SCCA2* promoter [11] has been reported, *SCCA1* promoter-driven oncolytic virotherapy has not. The present study is the first report of *SCCA1*-specific gene therapy. In clinical trials for squamous cell carcinoma, although adenovirus-*p53* for head and neck cancer [16], lung cancer [17], and esophageal cancer [18] and replicative oncolytic adenovirus for head and neck caner [19] have been reported, the results of such clinical trials were clinically insufficient because adenoviral infection was completely blocked by the production of anti-adenovirus antibody. This finding is identical to those for gene therapy with other viruses. It has been reported that oncolytic virus-infected carrier cells overcome the viral-induced humoral immune response, that the viral-induced cellular immune response kills virus-infected target cancer cells, and that granulocyte macrophage colony-stimulating factor augments the antitumor effect of carrier cells [14]. The present study also demonstrated that oncolytic adenovirus-infected A549 carrier cells induced elimination of tumor and that adenovirus-*GM-CSF* augmented the antitumor effect

DOI: 10.1002/jgm

of carrier cells, which induced complete regression of tumor in 90% of mice. Furthermore, a second challenge of syngeneic mouse squamous cell carcinoma was completely rejected by a specific antitumor response, also suggesting that the systemic tumor immune response induced by carrier cell treatment may cure not only carrier cell-injected local tumors, but also non-injected metastatic tumors. In conclusion, *SCCA1* promoter-driven oncolytic adenovirus-infected carrier cells may cure human squamous cell carcinoma of the head and neck, skin, oesophagus, lung, cervix, and other organs, and human clinical trials of these squamous cell carcinoma-specific carrier cells should be possible in the near future.

Acknowledgements

This study was supported by a grant from the Ministry of Education, Science, Sports and Culture, Japan, and by the Integrated Center for Science, Ehime University. We thank K. Oka for preparing culture medium and S. Hirose for comments and discussion. The authors have no conflicting financial interests to declare.

References

1. Takeshima N, Suminami Y, Takeda O, Abe H, Okuno N, Kato H. Expression of mRNA of SCC antigen in squamous cells. *Tumor Biol* 1992; **13**: 338–342.
2. Kato H, Torigoe H. Radioimmunoassay for tumor antigen of human cervical squamous cell carcinoma. *Cancer* 1977; **40**: 1621–1628.
3. Senekjian EK, Young JM, Weiser PA, Spencer CE, Magic SE, Herbst AL. An evaluation of squamous cell carcinoma antigen in patients with cervical squamous cell carcinoma. *Am J Obstet Gynecol* 1987; **157**: 433–439.
4. Bolli JA, Doering DL, Bosscher JR, *et al.* Squamous cell carcinoma antigen: clinical utility in squamous cell carcinoma of the uterine cervix. *Gynecol Oncol* 1994; **55**: 169–173.
5. Duk JM, de Bruijn HXA, Groenier KH, *et al.* Cancer of the uterine cervix: sensitivity and specificity of serum squamous cell carcinoma antigen determinations. *Gynecol Oncol* 1990; **39**: 186–194.
6. Takeshima N, Hirai Y, Katase K, Yano K, Yamauchi K, Hasumi K. The value of squamous cell carcinoma antigen as a predictor of nodal metastasis in cervical cancer. *Gynecol Oncol* 1998; **68**: 263–266.
7. Schneider SS, Schick C, Fish KE, *et al.* A serine proteinase inhibitor locus at 18q21.3 contains a tandem duplication of the human squamous cell carcinoma antigen gene. *Proc Natl Acad Sci USA* 1995; **92**: 3147–3151.
8. Hamada K, Shinomiya H, Asano Y, *et al.* Molecular cloning of human squamous cell carcinoma antigen 1 gene and characterization of its promoter. *Biochim Biophys Acta* 2001; **91522**: 1–8.
9. Sakaguchi Y, Kishi F, Murakami A, Suminami Y, Kato H. Structural analysis of human SCC antigen 2 promoter. *Biochim Biophys Acta* 1999; **1444**: 111–116.
10. Hamada K, Hanakawa Y, Hashimoto K, *et al.* Gene expression of human squamous cell carcinoma antigens 1 and 2 in human cell lines. *Oncol Rep* 2001; **8**: 347–54.
11. Hsu KF, Wu CL, Huang SC, *et al.* Conditionally replicating E1B-deleted adenovirus driven by the squamous cell carcinoma antigen 2 promoter for uterine cervical cancer therapy. *Cancer Gene Ther* 2008; **15**: 526–534.
12. Hamada K, Kohno S, Iwamoto M, *et al.* Identification of the human IAI.3B promoter element and its use in the construction of a replication-selective adenovirus for ovarian cancer therapy. *Cancer Res* 2003; **63**: 2506–2512.
13. Latham JPF, Searle PF, Mautner V, James ND. Prostate-specific antigen promoter/enhancer driven gene therapy for prostate cancer: construction and testing of a tissue-specific adenovirus vector. *Cancer Res* 2000; **60**: 334–341.
14. Hamada K, Desaki J, Nakagawa K, Shirakawa T, Gotoh A, Tagawa M. Carrier cell-mediated infection of a replication-competent adenovirus for cancer gene therapy. *Mol Ther* 2007; **15**: 1121–1128.
15. Suminami Y, Kishi F, Nawata S, *et al.* Promoter analyses of SCC antigen genes. *Biochim Biophys Acta* 2005; **1727**: 208–212.
16. Clayman GL, el-Naggar AK, Lippman SM, *et al.* Adenovirus-mediated p53 gene transfer in patients with advanced recurrent head and neck squamous cell carcinoma. *J Clin Oncol* 1998; **16**: 2231–2232.
17. Fujiwara T, Tanaka N, Kanazawa S, *et al.* Multicenter phase I study of repeated intratumoral delivery of adenoviral p53 in patients with advanced non-small-cell lung cancer. *J Clin Oncol* 2006; **24**: 1689–1699.
18. Shimada H, Matsubara H, Shiratori T, *et al.* Phase I/II adenoviral p53 gene therapy for chemoradiation resistant advanced esophageal squamous cell carcinoma. *Cancer Sci* 2006; **97**: 554–561.
19. Nemunaitis J, Khuri F, Ganly I, *et al.* Phase II trial of intratumoral administration of ONYX-015, a replication-selective adenovirus, in patients with refractory head and neck cancer. *J Clin Oncol* 2001; **19**: 289–298.

QUERIES TO BE ANSWERED BY AUTHOR

IMPORTANT NOTE: Please mark your corrections and answers to these queries directly onto the proof at the relevant place. Do NOT mark your corrections on this query sheet.

Queries from the Copyeditor:

AQ1 '3000 r.p.m.'. Please provide '*g*' value

AQ2 'LIFETEST procedure'. Please provide the details of any software package used (i.e. manufacturer and manufacturer's location or a URL from where it can be obtained)

British Journal of Cancer (2010) 102, 206–212

www.bjcancer.com

Gene set enrichment analysis provides insight into novel signalling pathways in breast cancer stem cells

M Murohashi[1,6], K Hinohara[1,6], M Kuroda[2], T Isagawa[3], S Tsuji[3], S Kobayashi[4], K Umezawa[5], A Tojo[4], H Aburatani[3] and N Gotoh[*,1]

[1]Division of Systems Biomedical Technology, Institute of Medical Science, University of Tokyo, Tokyo, Japan; [2]Department of Pathology, Tokyo Medical University, Tokyo, Japan; [3]Genome Science Division, Research Center of Advanced Science and Technology, University of Tokyo, Tokyo, Japan; [4]Division of Molecular Therapy, Institute of Medical Science, University of Tokyo, Tokyo, Japan; [5]Department of Applied Chemistry, Faculty of Science and Technology, Keio University, Yokohama, Japan

BACKGROUND: Tumour-initiating cells (TICs) or cancer stem cells can exist as a small population in malignant tissues. The signalling pathways activated in TICs that contribute to tumourigenesis are not fully understood.

METHODS: Several breast cancer cell lines were sorted with CD24 and CD44, known markers for enrichment of breast cancer TICs. Tumourigenesis was analysed using sorted cells and total RNA was subjected to gene expression profiling and gene set enrichment analysis (GSEA).

RESULTS: We showed that several breast cancer cell lines have a small population of $CD24^{-/low}/CD44^{+}$ cells in which TICs may be enriched, and confirmed the properties of TICs in a xenograft model. GSEA revealed that $CD24^{-/low}/CD44^{+}$ cell populations are enriched for genes involved in transforming growth factor-β, tumour necrosis factor, and interferon response pathways. Moreover, we found the presence of nuclear factor-κB (NF-κB) activity in $CD24^{-/low}/CD44^{+}$ cells, which was previously unrecognised. In addition, NF-κB inhibitor dehydroxymethylepoxyquinomicin (DHMEQ) prevented tumourigenesis of $CD24^{-/low}/CD44^{+}$ cells *in vivo*.

CONCLUSION: Our findings suggest that signalling pathways identified using GSEA help to identify molecular targets and biomarkers for TIC-like cells.

British Journal of Cancer (2010) **102,** 206–212. doi:10.1038/sj.bjc.6605468 www.bjcancer.com
Published online 8 December 2009

Keywords: tumour-initiating cells; NF-κB; CD24; CD44; gene expression profiling; DHMEQ

Accumulating evidence suggests that tumour-initiating cells (TICs) or cancer stem cells—which make up only a small proportion of heterogeneous tumour cells—possess a greater ability to maintain tumour formation than other tumour cell types. It has been proposed that TICs have characteristics in common with normal stem cells from tumour-prone tissue (Ailles and Weissman, 2007). For instance, TICs can self-renew and simultaneously produce differentiated daughter cells that proliferate strongly until they reach their final differentiated state. Apparent differences also exist between TICs and normal stem cells. The latter are maintained under tight homoeostatic regulation and are passively protected in the surrounding microenvironment or stem cell niche in adult tissues. However, the former may actively contribute to tumour formation. Although the concept of TICs greatly influences cancer biology and evokes a reconsideration of cancer treatment, the molecular mechanisms involved in the contribution of TICs to tumourigenesis remain obscure.

In human breast cancers, a population characterised by the expression of cell-surface markers, $CD24^{-/low}/CD44^{high}$, was reported to be highly enriched in TICs, compared with populations of $CD24^{high}/CD44^{high}$ cells (Al-Hajj *et al*, 2003; Mani *et al*, 2008). Two gene-expression profiling studies, comparing $CD24^{-/low}/CD44^{+}$ cell populations with other populations in primary breast cancer cells or in normal tissue, presented the $CD24^{-/low}/CD44^{+}$ cell population-derived different signatures that seemed to predict poorer prognosis (Liu *et al*, 2007; Shipitsin *et al*, 2007). One study showed that transforming growth factor (TGF)-β pathways seem to be activated in these cells (Shipitsin *et al*, 2007). It was subsequently reported that TGF-β induced the epithelial–mesenchymal transition (EMT) in mammary glands and stem-like cells in both normal mammary epithelial cells and breast cancer cells (Mani *et al*, 2008). Because TGF-β signalling can have positive or negative effects on tumourigenesis, additional signalling may still be needed to stimulate tumourigenesis.

Nuclear factor-κB (NF-κB) is a transcription factor complex and is typically a heterodimer of p50, p52, p65 (RelA), RelB, and c-Rel. It is usually inactive and bound to IκB, an inhibitory protein, in the cytoplasm. Upon stimulation with signals such as tumour

*Correspondence: Dr N Gotoh, Division of Systems Biomedical Technology, Institute of Medical Science, University of Tokyo, Tokyo, Japan; E-mail: ngotoh@ims.u-tokyo.ac.jp
[6]These authors contributed equally to this work.
Received 10 August 2009; revised 26 October 2009; accepted 9 November 2009; published online 8 December 2009

necrosis factor (TNF) or interferon (INF), IκB is first phosphorylated, then ubiquitinated, and finally degraded. Released NF-κB translocates to the nucleus and binds to the κB sequence, wherein it promotes the transcription of various genes, including inflammatory cytokines. Nuclear factor-κB is involved in inflammation, angiogenesis, inhibition of apoptosis, and tumourigenesis (Karin *et al*, 2002; Huber *et al*, 2004; Tabruyn and Griffioen, 2008).

Gene set enrichment analysis (GSEA) is a recently developed analytical method of gene-expression profiling. The results are easier to interpret biologically, and the method is more accurate and robust than individual gene analysis methods, such as fold change analysis of expression levels (Subramanian *et al*, 2005).

In this study, we effectively used GSEA to comprehensively analyse signalling pathways in TICs using breast cancer cell lines. As a result, we identified multiple signalling pathways potentially activated in TIC-like cells, including both known and unknown pathways. We found activity of NF-κB, which was previously unrecognised, in TIC-like cells. Therefore, it is possible that the signalling pathways identified using GSEA help to identify novel candidates of molecular targets that have important roles in tumourigenesis in human breast cancer TICs.

MATERIALS AND METHODS

Cell culture

Breast cancer cell lines HCC70, HCC1954, MCF7, SK-BR-3, AU-565, BT-474, T-47D, and MDA-MB-231 were purchased from the American Type Culture Collection (ATCC, Manassas, VA, USA). Cells were cultured according to the manufacturer's instructions.

FACS

Cells were sorted or analysed after staining with CD24-FITC or CD44-PE antibody (BD Pharmingen, San Jose, CA, USA), and dead cells were eliminated using propidium iodide (Sigma, Saint Louis, MO, USA) and FACS VantageSE (BD Biosciences, Bedford, MA, USA). Data were analysed by FlowJo 7.2.2 Tree Star Inc. Ashland, OR, USA.

Construction of lentiviral vectors

A third-generation self-inactivating lentiviral transfer vector plasmid with a gene encoding firefly luciferase or d2Venus (Nagai *et al*, 2002) (provided by Dr A Miyawaki, RIKEN, Wako, Japan) under the control of the elongation factor 1-α (EF1α) promoter was produced using constructs provided by Dr H Miyoshi (RIKEN, Tsukuba, Japan) by standard molecular biological techniques (Miyoshi *et al*, 1999). These vectors also contained the central polypurine track and the woodchuck hepatitis virus post-regulatory element. Viral supernatant was produced by transient transfection of 293T cells with packaging plasmids (pMDLg/p.RRE) and HIV rev expression plasmids (pRSV-rev) and was then pseudotyped with the vesicular stomatitis virus G protein (pMD.G), as previously described (Bai *et al*, 2003). High-titre viral stocks were prepared by ultracentrifugation. The functional titres of these vectors (HIV-EF1α-Luciferase, HIV-EF1α-d2Venus) were determined by infection of HeLa cells using a real-time PCR method (DNA titre; Sastry *et al*, 2002). All the multiplicity of infection (MOI) values used in our experiments were calculated from DNA titres.

Transduction of cells with lentiviral vectors

HCC1954 and MCF7 cells were pelleted and incubated with viral supernatant at an MOI of 10 in a 1.5-ml Eppendorf tube. After incubation for 2 h at 37°C in 5% CO_2, cells were cultured until they were used in *in vivo* experiments. Because HIV-EF1a-d2Venus was used for confirmation of transduction efficiency, HIV-EF1a-Luciferase and HIV-EF1a-d2Venus were infected simultaneously in separate tubes. After more than three passages, the cells were used for FACS analysis or in the xenograft model.

Xenografts

Six-week-old female NOD/SICD mice were anaesthetised with isoflurane (Abbott Japan, Tokyo, Japan), and then 0.72 mg, 60-day-release β-estradiol (E2) pellets (Innovative Research of America, Sarasota, FL, USA) were implanted s.c. on the back of the neck (only in the case of MCF7 implantation). A total of 1×10^2 to 3×10^4 sorted cells were suspended in 1 : 1 volumes of phosphate-buffered saline (PBS)(−)/Matrigel (BD Biosciences) to produce 100 μl of mixture and were then injected into the mammary fat pads. Dehydroxymethylepoxyquinomicin (DHMEQ) was suspended in 0.5% chloromethyl cellulose and administrated by i.p. injections of 100 μl containing 12 mg kg^{-1} thrice a week. Control groups were injected with the same volume of vehicle. All treatments started on day 2 after tumour cell implantation.

Mice were handled according to the guidelines of the Institute of Medical Science, University of Tokyo. The experiments were approved by the committee for animal research at the institution.

In vivo imaging

Mice under anaesthesia were injected i.p. with 150 mg kg^{-1} of luciferin (Promega, Madison, WI, USA) in PBS(−), and images were recorded by the IVIS Imaging System (Xenogen, Hopkington, MA, USA) 5 min after the injection. The bioluminescence images were quantified by Living Image software (Xenogen). Observations by IVIS were continued once a week, immediately after the injection, up to 4 weeks. In DHMEQ treatment, tumour growth was monitored by luciferase activity twice a week, for up to 32 days.

Histology analysis

Tumours from xenograft cells were fixed in 10% neutralised buffered formalin, embedded in paraffin, and then stained with haematoxylin–eosin (HE).

Microarray analysis

For microarray analysis, 1% of the entire population of the HCC1954, MCF7, or HCC70 cell line, belonging to $CD24^-CD44^+$, was purified on the basis of the lowest expression levels of CD24. In addition ten percent of the entire cell population of each cell line, belonging to $CD24^+/CD44^+$, was purified as the control population ($CD24^+$). There was no significant difference in tumourigenicity, whether we considered 1 or 10% of the entire $CD24^{-/low}/CD44^+$ population as the TIC population. Microarray analyses were performed as previously described (Morikawa *et al*, 2007). Briefly, total RNA was isolated from samples using TRIzol (Invitrogen, Carlsbad, CA, USA) according to the manufacturer's instructions. Six samples were analysed on an Affymetrix high-density oligonucleotide array, Human Genome U133 Plus 2.0. Output images were processed by the MAS5 algorithm and globally scaled to a target intensity of 100. To identify gene-signature-based differences between $CD24^{-/low}/CD44^+$ and $CD24^+/CD44^+$ populations, we performed GSEA (Subramanian *et al*, 2005). All probe sets were pre-ranked using the ratio of the geometric mean of each group's expression values; thereafter, the ordered probe set list was used as the GSEA input. The detailed GSEA parameters are as follows: the number of permutations is 2500, and the permutation

type is configured to the gene set to avoid the potential problem of a small sample size.

Quantification of NF-κB activity

Nuclear extracts were prepared with a Nuclear Extract Kit according to the manufacturer's instructions (Active Motif, Carlsbad, CA, USA). Briefly, $CD24^{-/low}/CD44^{+}$ and $CD24^{+}/CD44^{+}$ populations were sorted from the bulk of HCC1954 or MCF7 cells and isolated from the nuclear extracts. NF-κB p65 activity was measured with a TransAM NF-κB p65 Transcription Factor Assay kit (Active Motif) according to the manufacturer's instructions. Four sets of nuclear extracts from each population were prepared, and 20 μg of each extract was used for the p65 NF-κB activity assay.

RESULTS

TIC populations in breast cancer cell lines

To examine whether $CD24^{-/low}/CD44^{+}$ cell populations exist in various types of breast cancer cell lines, we analysed the expression of these surface markers in eight breast cancer cell lines by FACS analysis (Figure 1). We found that each cell line had various expression levels of CD24 and CD44. HCC1954, MCF7, HCC70, and MDA-MB-231 cells had relatively high percentages of $CD44^{+}$ cell populations, whereas BT-474, AU-565, SK-BR-3, and T47-D cells showed low CD44 expression levels. HCC1954, MCF7, and HCC70 cells had a small population of $CD24^{-/low}/CD44^{+}$ cells. This situation might be similar to that in early-stage breast cancer tissues in which the TIC population is assumed to be small. To determine the hierarchical organisation of breast cancer cell lines, we analysed the tumourigenic potential of the $CD24^{-/low}/CD44^{+}$ and $CD24^{+}/CD44^{+}$ cell populations of HCC1954 and MCF7 cell lines.

Tumourigenicity of $CD24^{-/low}/CD44^{+}$ cell populations in breast cancer cell lines

The *in vivo* tumourigenicity assay is the gold standard for identifying TICs (Clarke *et al*, 2006). Tumourigenicity of TICs has been examined by using NOD/SCID mouse and measuring palpable tumours. To improve the quality of the quantitative results, we used *in vivo* bioluminescence imaging (IVIS) to measure tumour growth. We first transduced cells with a lentiviral vector encoding luciferase or d2Venus (an improved version of yellow fluorescent protein) cDNA. We measured transduction efficiency by expression levels of d2Venus using FACS. As shown in Supplementary Figure 1, high transduction efficiency was obtained in each cell line: 92.60 and 99.29% for HCC1954 and MCF7 cells, respectively. Next, we transduced a lentiviral vector expressing luciferase into these cells. Because we used similar MOI levels for transduction of the lentiviral vectors expressing luciferase and d2Venus, we expected similar levels of luciferase expression in each cell line. These were designated HCC1954-Luc or MCF7-Luc. Cells in $CD24^{-/low}/CD44^{+}$ populations were considered to be enriched for TICs, and $CD24^{+}CD44^{+}$ populations were used as controls. We compared the expression levels of luciferase in both cell populations and confirmed that there were no significant differences (Supplementary Figure 2).

Cells were implanted into mammary fat pads of NOD/SCID mice and tumour growth was measured by quantifying luciferase activity using the IVIS Imaging System. A total of 10 000 HCC1954-Luc and MCF7-Luc cells of both populations were implanted (Figure 2A and C). After 4 weeks, the analysis of luciferase activity indicated that cells in the $CD24^{-/low}/CD44^{+}$ populations of HCC1954-Luc and MCF7-Luc generated significantly larger tumours than the control populations ($P<0.05$).

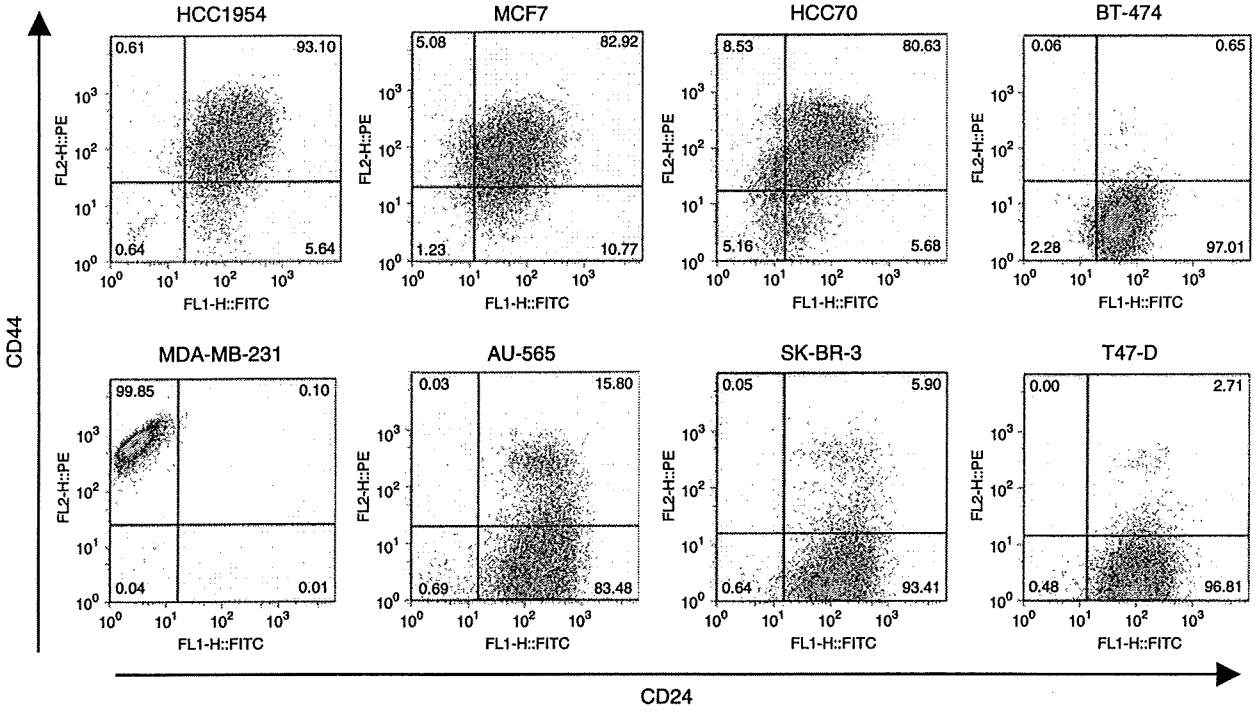

Figure 1 CD24 and CD44 expression patterns in breast cancer cell lines. Expression patterns of CD24 and CD44 in breast cancer cell lines (HCC1954, MCF7, HCC70, BT-474, MDA-MB-231, AU-565, SK-BR-3, and T-47D) were analysed by FACS. Anti-CD24 antibody labelled with FITC and anti-CD44 antibody labelled with PE were applied to the analysis. Gates are based on the isotype control corresponding to each cell line.

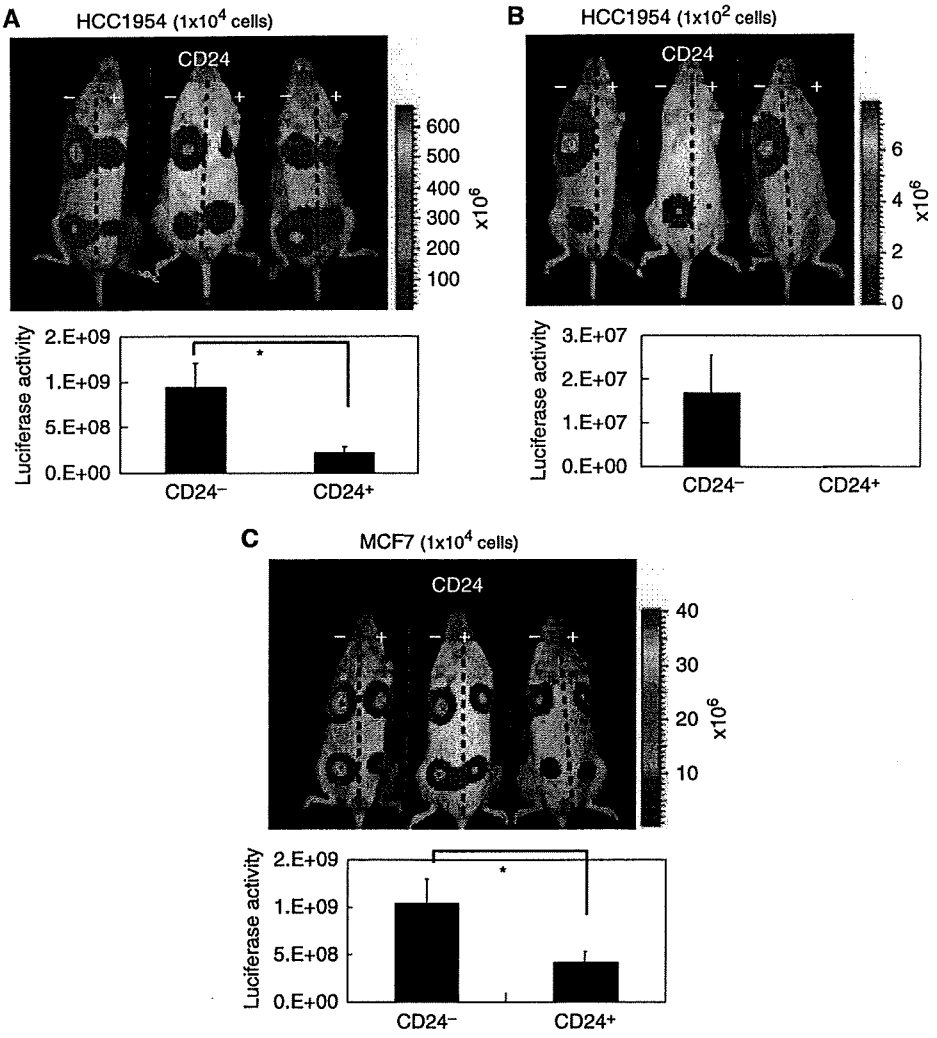

Figure 2 Luciferase activities of $CD24^{-/low}/CD44^+$ cells in NOD/SCID mice. HCC1954 and MCF7 cells expressing luciferase were sorted by FACS. Ten per cent of the entire population, belonging to $CD24^{-/low}$ $CD44^+$, was selected as the TIC population ($CD24^-$). Ten per cent of the whole population, belonging to $CD24^+/CD44^+$, was selected as the control ($CD24^+$). We transplanted both populations of 1×10^4 HCC1954 cells (**A**), 1×10^2 HCC1954 cells (**B**) of 1×10^4 CF7 cells (**C**) in mammary fat pads of NOD/SCID mice. Luciferase activities were captured by IVIS after 4 weeks (upper panels). Luciferase activities in implanted sites were quantified ($n = 6$) (lower graphs). Results are represented as mean ± s.d. $^*P < 0.05$ (Student's *t*-test).

Moreover, when we transplanted both populations of 1×10^2 HCC1954-Luc, we found that tumours were generated only by the $CD24^{-/low}/CD44^+$ population ($n = 6$) (Figure 2B).

These results indicate that $CD24^{-/low}/CD44^+$ populations in breast cancer cell lines have higher tumourigenicity than control populations. It is therefore likely that $CD24^{-/low}/CD44^+$ cells in breast cancer cell lines may behave in a manner similar to TICs.

We also examined the histology of tumours derived from HCC1954-Luc cells from both populations and from an unsorted population when 1×10^4 cells of each population were implanted. HE staining revealed that tumours derived from $CD24^{-/low}/CD44^+$ and unsorted cells showed a similar histology, namely, exclusively invasive patterns with a variety of morphologies and the stromal component (Supplementary Figure 3). In contrast, tumours derived from control cells showed both invasive and differentiated patterns associated with a smaller stromal component than $CD24^{-/low}/CD44^+$ or unsorted cells.

Gene-expression profiling and GSEA for the identification of pathways and key effectors in $CD24^{-/low}/CD44^+$ cells

To identify expressed genes that were highly enriched in $CD24^{-/low}/CD44^+$ and control cells, we performed DNA microarray analysis using HCC1954, MCF7, and HCC70 cell lines that have small populations of $CD24^-/CD44^+$ cells. To select cell populations strictly, we used only $CD24^-/CD44^+$ cell populations that accounted for approximately 1% of the entire population. As control, we used $CD24^+/CD44^+$ cell populations that comprised approximately 10% of the entire population. Microarray data were ranked by the expression ratio between the geometric mean of the $CD24^{-/low}/CD44^+$:$CD24^+/CD44^+$ populations from the three cell lines (Supplementary Table). We then applied GSEA (Subramanian *et al*, 2005). Our results showed that gene sets involving TGF-β pathways and oncogeneic Ras pathways were upregulated in $CD24^{-/low-}/CD44^+$ populations (Figure 3). Moreover, we found that both *TNF* and IFN response

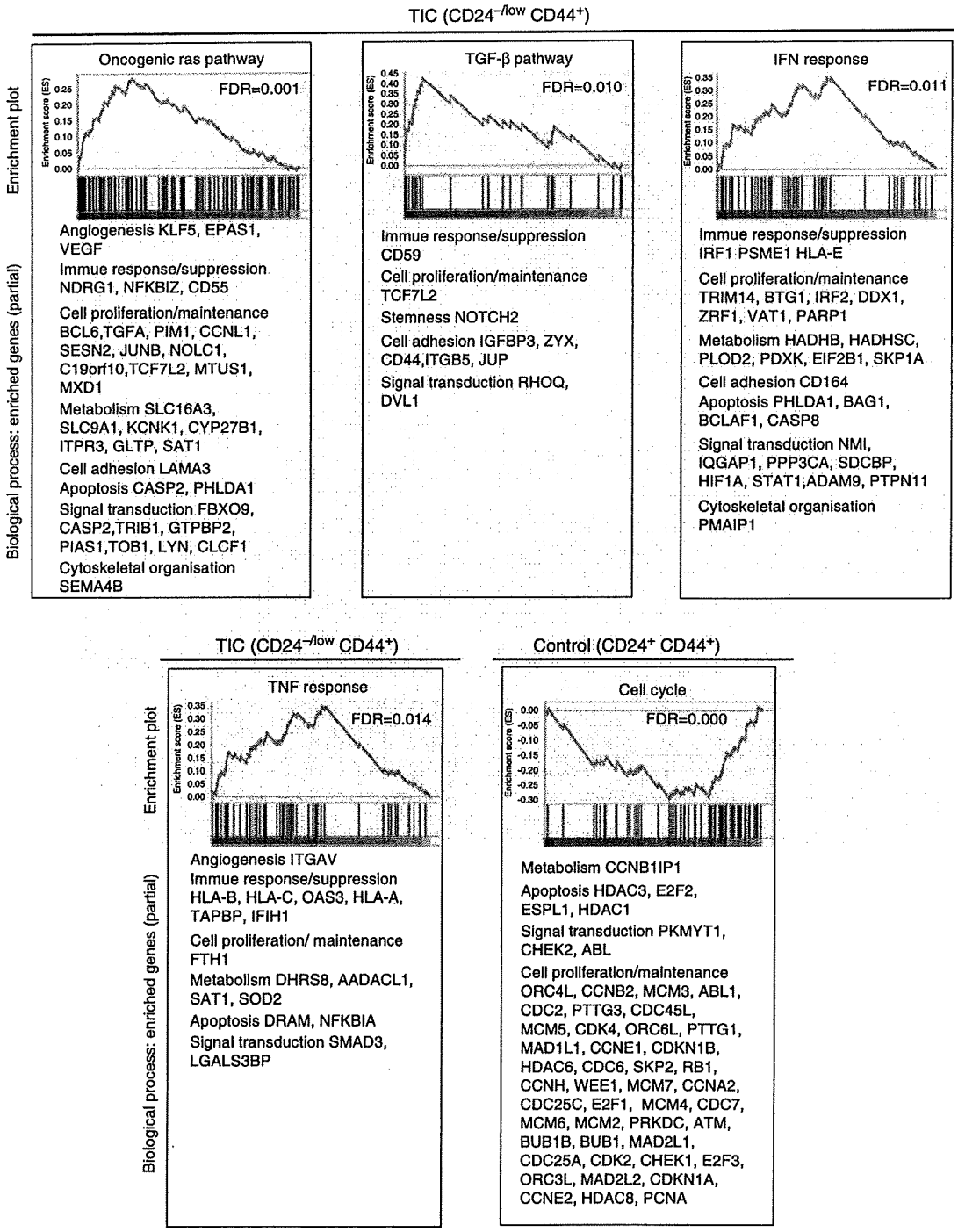

Figure 3 Gene set enrichment analysis. DNA microarray analyses were performed to compare TIC and control populations of HCC70, HCC1954, and MCF7. One per cent of the whole population of each cell line, belonging to $CD24^{-}/CD44^{+}$, purified on the basis of the lowest expression levels of CD24, was selected as the TIC population. Ten per cent of the whole population, belonging to $CD24^{+}/CD44^{+}$, was purified for the control. Microarray data were ranked using the geometric mean of the expression ratios between the TIC and control populations from the three cell lines, and GSEA was then applied. GSEA-extracted representative pathways containing genes enriched in the TIC or control populations are shown. In the original GSEA data sets, the oncogenic Ras pathway is depicted as RAS_ONCOGENIC_SIGNATURE, the TGF-β pathway is depicted as TGFBETA_ EARLY_UP, the IFN response is depicted as IFN_ANY_UP, and the TNF response pathway is depicted as SANA_TNFA_ENDOTHELIAL_UP.

gene signatures were markedly enriched in $CD24^{-/low-}/CD44^{+}$ populations.

With regard to individual genes, gene-ontology-based classification revealed that genes involved in 'stemness', cell proliferation/maintenance, cell adhesion, cell motility, invasion, angiogenesis, growth factor/cytokine, immune response/suppression, and metabolism were highly represented in $CD24^{-/low-}/CD44^{+}$ cells compared with control cell populations. All these genes may

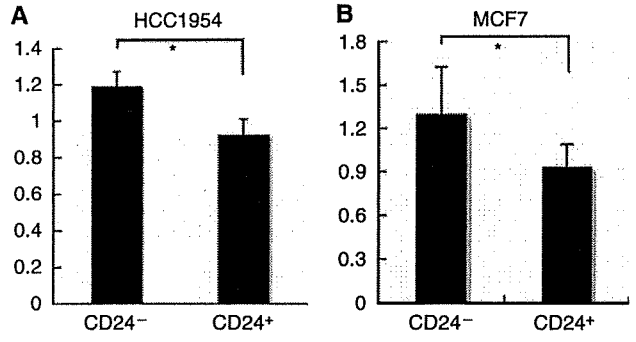

Figure 4 Activity of NF-κB. Quantification of NF-κB activity in $CD24^{-}$/$CD44^{+}$ and $CD24^{+}$/$CD44^{+}$ populations sorted from HCC1954 (**A**) and MCF7 cells (**B**). The data (mean ± s.d.) are representative of three experiments. $^{*}P<0.05$.

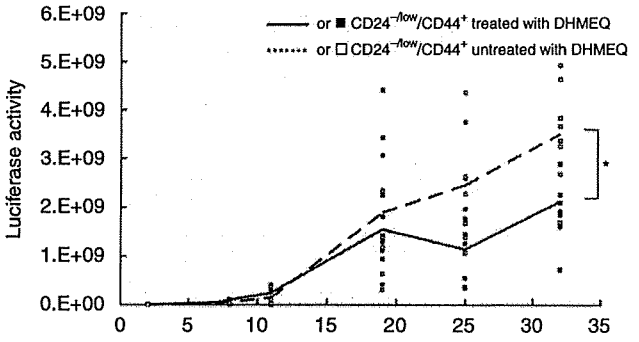

Figure 5 Effects on tumourigenesis after treatment with NF-κB inhibitor. Tumour growth of $CD24^{-/low}$/$CD44^{+}$ populations of HCC1954 cells treated with NF-κB inhibitor DHMEQ was measured by luciferase activity ($n=8$). Averages of luciferase activity are indicated by lines. $^{*}P<0.05$.

contribute to oncogenesis. For example, from the GSEA results, we found *Notch2*, a 'stemness'-related gene, in the TGF-β pathway; *LAMA3*, a cell invasion- or adhesion-related gene, in the oncogenic Ras pathway; and *KLF5*, *EPAS1*, and *VEGF*, angiogenesis-related genes, in the oncogenic Ras pathway (Figure 3, in red). Conversely, GSEA revealed that genes highly expressed in control populations correlated with several cell-cycle-associated gene sets, which have large numbers of cell proliferation/maintenance-related genes.

One of the important effector molecules common to both TNF and IFN response pathways is NF-κB. We quantified NF-κB activities in nuclear extracts of $CD24^{-/low}$/$CD44^{+}$ and control populations that were sorted by FACS analysis. We found that the activity of NF-κB was significantly higher in $CD24^{-/low}$/$CD44^{+}$ than in $CD24^{+}$/$CD44^{+}$ populations (Figure 4).

The TNF or IFN response pathway is involved in the expression of many inflammatory cytokines/chemokines. Vascular endothelial growth factor A, interleukin 8, and chemokine (C-C motif) ligand 5 are among the inflammatory cytokines/chemokines associated with stroma-like activities (Shono *et al*, 1996; Moriuchi *et al*, 1997; Yoshida *et al*, 1997; Cho *et al*, 2007). Among the highly ranked genes, we also noticed Toll-like receptor 1, another upstream activator for NF-κB, and stromal cell-derived factor 2-like 1, which is reported to be upregulated through EMT, an important biological output of the TGF-β pathway (Massagué, 2008; Sarrio *et al*, 2008; Rakoff-Nahoum and Medzhitov, 2009). We measured the expression levels of these genes by quantitative RT-PCR and confirmed that they were expressed at significantly higher levels in $CD24^{-/low-}$/$CD44^{+}$ populations compared with control cells (Supplementary Figure 4).

Decreased tumourigenesis in $CD24^{-/low}$/$CD44^{+}$ populations after treatment with DHMEQ, a specific inhibitor for NF-κB

We next examined the role of NF-κB activity in tumourigenesis using a mouse model. TICs are believed to be important at the beginning of tumourigenesis or in its recurrence; therefore, we analysed tumourigenesis at early points from relatively small numbers of TIC-like cells. We transplanted 10^4 cells of $CD24^{-/low}$/$CD44^{+}$ populations into NOD/SCID mice, as shown in Figure 2, and treated them with DHMEQ, a specific inhibitor for NF-κB (Umezawa, 2006; Supplementary Results; Supplementary Figures 5 and 6). To analyse the effects occurring during the course of tumourigenesis, we began inhibitor treatment 2 days after transplantation. We monitored tumour formation by *in vivo* imaging and found that the luciferase activities of the tumours derived from $CD24^{-/low}$/$CD44^{+}$ cell populations treated with DHMEQ were significantly decreased compared with that of untreated cell-derived tumours (Figure 5). This finding suggests that NF-κB functions as a key effector of tumourigenesis derived from TIC-like cells.

DISCUSSION

In this study, we established a mouse model that may recapitulate part of the tumourigenic process in TICs, using breast cancer cell lines. We showed that cells derived from $CD24^{-/low}$/$CD44^{+}$ populations resulted in tumours larger than those of $CD24^{+}$/$CD44^{+}$ control populations. Importantly, when as few as 100 cells were implanted, only $CD24^{-/low}$/$CD44^{+}$ populations gave rise to tumours (Figure 2B). This is an important criterion for TICs (Clarke *et al*, 2006). Therefore, the $CD24^{-/low}$/$CD44^{+}$ populations in cell lines may be enriched with TIC-like cells. Our results revealed heterogeneity in cell populations divided into TIC-like cells and other cells. Consistent with our data, it has been recently reported that other cell lines also have TIC-like cell populations (Fillmore and Kuperwasser, 2008). Therefore, it is reasonable to assume that several breast cancer cell lines are heterogeneous and that they have distinct cell populations: TIC-like cells and other cells, with both cell types preserving the characteristics of TICs and other cells in primary cancer tissues to some extent.

Moreover, we labelled cells with a luciferase reporter gene and established a monitoring system of tumourigenesis in the fat pads of NOD/SCID mice by sensitive and quantitative *in vivo* imaging that can detect as few as 100 cells. Because TICs are thought to be important in tumourigenesis during transition from the pre-malignant stage to the malignant stage or during recurrence with a few tumour cells, this model should be useful for monitoring tumourigenesis at these stages. Indeed, we were able to validate candidate targets in TICs using inhibitors for NF-κB in our model (Figure 5).

Gene-expression profiling combined with GSEA showed that several signalling pathways and genes are involved in $CD24^{-/low}$/$CD44^{+}$ TIC-like cells compared with $CD24^{+}$/$CD44^{+}$ control populations. Gene Ontology Classification revealed that a variety of genes may represent malignant characteristics of $CD24^{-/low}$/$CD44^{+}$ TIC-like cells. There is an overlap with those genes found in a previous report using cells from $CD24^{-/low}$/$CD44^{+}$ and $CD24^{+}$/$CD44^{+}$ populations derived from normal breast and primary breast cancer tissues. Some genes involved in the TGF-β pathway were enriched in $CD24^{-/low}$/$CD44^{+}$ populations, consistent with the previous report (Shipitsin *et al*, 2007). Importantly, we found genes associated with oncogenic Ras pathways, as well as with TNF and IFN response pathways, as novel gene sets in $CD24^{-/low}$/$CD44^{+}$ populations. It is likely that genes involved in the oncogenic Ras pathway, the TNF response pathway, and the

IFN response pathway are specifically represented in TICs but not in normal stem cells.

The TGF-β pathway inhibits tumourigenesis when it is the only pathway activated in cells (Massagué, 2008). However, in the malignant state, the TGF-β pathway cooperates with other pathways to facilitate tumourigenesis. It has been reported that the oncogenic Ras pathway, inflammatory responses, and activation of NF-κB are such cooperative pathways (Huber *et al*, 2004).

These findings suggest that TICs are more malignant than other cells in cancer. We also cannot rule out the possibility that cell lines may have additional characteristics that differ from those of primary cells. For example, cell-cycle-related gene sets found to be enriched in control cells may somehow reflect *in vitro* culture adaptations (Figure 3). The enhanced cell-cycling activity might allow control cells to grow *in vivo* after implantation; whereas control cells derived from primary tissues rarely generate tumours *in vivo* (Figure 2).

We showed that activity of NF-κB is higher in TIC-like cells than in control cells. Moreover, DHMEQ, a highly specific inhibitor for NF-κB, suppressed tumourigenesis in the TIC-like cells in our mouse model. This was assessed following treatment that occurred soon after transplantation. Thus, NF-κB could be a promising target for treatment of early stages of breast cancer and for the prevention of recurrence.

Taken together, our findings raise an intriguing possibility: TICs behave in a manner similar to CAFs and can actively generate and maintain the cancer stem cell niche, in which NF-κB functions as the main effector that can induce many secretory proteins, including cytokines and chemokines. Future studies should focus on the extensive evaluation of our model by using clinical samples of breast cancer.

ACKNOWLEDGEMENTS

We thank Dr Nobukazu Watanabe and Ms Yumiko Ishii for consulting and manipulating the Flow cytometer. We thank Dr Yusuke Inoue for giving us technical advice about IVIS operation. This work was supported by grants from the Ministry of Education, Culture, Sports, Science and Technology of Japan; Ministry of Health, Labor and Welfare of Japan for the third-term Comprehensive 10-year Strategy for Cancer Control; Ministry of Health, Labor and Welfare of Japan for Cancer research; Naito Foundation; and Cell Science Research Foundation.

Supplementary Information accompanies the paper on British Journal of Cancer website (http://www.nature.com/bjc)

REFERENCES

Ailles LE, Weissman IL (2007) Cancer stem cells in solid tumors. *Curr Opin Biotechnol* **18:** 460–466

Al-Hajj M, Wicha MS, Benito-Hernandez A, Morrison SJ, Clarke MF (2003) Prospective identification of tumorigenic breast cancer cells. *Proc Natl Acad Sci USA* **100:** 3983–3988

Bai Y, Soda Y, Izawa K, Tanabe T, Kang X, Tojo A, Hoshino H, Miyoshi H, Asano S, Tani K (2003) Effective transduction and stable transgene expression in human blood cells by a third-generation lentiviral vector. *Gene Therapy* **10:** 1446–1457

Cho ML, Ju JH, Kim HR, Oh HJ, Kang CM, Jhun JY, Lee SY, Park MK, Min JK, Park SH, Lee SH, Kim HY (2007) Toll-like receptor 2 ligand mediates the upregulation of angiogenic factor, vascular endothelial growth factor and interleukin-8/CXCL8 in human rheumatoid synovial fibroblasts. *Immunol Lett* **108:** 121–128

Clarke MF, Dick JE, Dirks PB, Eaves CJ, Jamieson CH, Jones DL, Visvader J, Weissman IL, Wahl GM (2006) Cancer stem cells—perspectives on current status and future directions: AACR Workshop on cancer stem cells. *Cancer Res* **66:** 9339–9344

Fillmore CM, Kuperwasser C (2008) Human breast cancer cell lines contain stem-like cells that self-renew, give rise to phenotypically diverse progeny and survive chemotherapy. *Breast Cancer Res* **10:** R25

Huber MA, Beug H, Wirth T (2004) Epithelial–mesenchymal transition: NF-kappaB takes center stage. *Cell Cycle* **3:** 1477–1480

Karin M, Cao Y, Greten FR, Li ZW (2002) NF-kappaB in cancer: from innocent bystander to major culprit. *Nat Rev Cancer* **2:** 301–310

Liu R, Wang X, Chen GY, Dalerba P, Gurney A, Hoey T, Sherlock G, Lewicki J, Shedden K, Clarke MF (2007) The prognostic role of a gene signature from tumorigenic breast-cancer cells. *N Engl J Med* **356:** 217–226

Mani SA, Guo W, Liao MJ, Eaton EN, Ayyanan A, Zhou AY, Brooks M, Reinhard F, Zhang CC, Shipitsin M, Campbell LL, Polyak K, Brisken C, Yang J, Weinberg RA (2008) The epithelial–mesenchymal transition generates cells with properties of stem cells. *Cell* **133:** 704–715

Massagué J (2008) TGFβ in Cancer. *Cell* **134:** 215–230

Miyoshi H, Smith KA, Mosier DE, Verma IM, Torbett BE (1999) Transduction of human CD34$^+$ cells that mediate long-term engraftment of NOD/SCID mice by HIV vectors. *Science* **283:** 682–686

Morikawa T, Sugiyama A, Kume H, Ota S, Kashima T, Tomita K, Kitamura T, Kodama T, Fukayama M, Aburatani H (2007) Identification of Toll-like receptor 3 as a potential therapeutic target in clear cell renal cell carcinoma. *Clin Cancer Res* **13:** 5703–5709

Moriuchi H, Moriuchi M, Fauci AS (1997) Nuclear factor-kappa B potently up-regulates the promoter activity of RANTES, a chemokine that blocks HIV infection. *J Immunol* **158:** 3483–3491

Nagai T, Ibata K, Park ES, Kubota M, Mikoshiba K, Miyawaki A (2002) A variant of yellow fluorescent protein with fast and efficient maturation for cell-biological applications. *Nat Biotechnol* **20:** 87–90

Rakoff-Nahoum S, Medzhitov R (2009) Toll-like receptors and cancer. *Nat Rev Cancer* **9:** 57–63

Sarrio D, Rodriguez-Pinilla SM, Hardisson D, Cano A, Moreno-Bueno G, Palacios J (2008) Epithelial–mesenchymal transition in breast cancer relates to the basal-like phenotype. *Cancer Res* **68:** 989–997

Sastry L, Johnson T, Hobson MJ, Smucker B, Cornetta K (2002) Titering lentiviral vectors: comparison of DNA, RNA and marker expression methods. *Gene Therapy* **9:** 1155–1162

Shipitsin M, Campbell LL, Argani P, Weremowicz S, Bloushtain-Qimron N, Yao J, Nikolskaya T, Serebryiskaya T, Beroukhim R, Hu M, Halushka MK, Sukumar S, Parker LM, Anderson KS, Harris LN, Garber JE, Richardson AL, Schnitt SJ, Nikolsky Y, Gelman RS, Polyak K (2007) Molecular definition of breast tumor heterogeneity. *Cancer Cell* **11:** 259–273

Shono T, Ono M, Izumi H, Jimi SI, Matsushima K, Okamoto T, Kohno K, Kuwano M (1996) Involvement of the transcription factor NF-kappaB in tubular morphogenesis of human microvascular endothelial cells by oxidative stress. *Mol Cell Biol* **16:** 4231–4239

Subramanian A, Tamayo P, Mootha VK, Mukherjee S, Ebert BL, Gillette MA, Paulovich A, Pomeroy SL, Golub TR, Lander ES, Mesirov JP (2005) Gene set enrichment analysis: a knowledge-based approach for interpreting genome-wide expression profiles. *Proc Natl Acad Sci USA* **102:** 15545–15550

Tabruyn SP, Griffioen AW (2008) NF-kappa B: a new player in angiostatic therapy. *Angiogenesis* **11:** 101–106

Umezawa K (2006) Inhibition of tumor growth by NF-kappaB inhibitors. *Cancer Sci* **97:** 990–995

Yoshida S, Ono M, Shono T, Izumi H, Ishibashi T, Suzuki H, Kuwano M (1997) Involvement of interleukin-8, vascular endothelial growth factor, and basic fibroblast growth factor in tumor necrosis factor alpha-dependent angiogenesis. *Mol Cell Biol* **17:** 4015–4023

Human Reproduction, Vol.24, No.6 pp. 1359–1372, 2009
Advanced Access publication on February 27, 2009 doi:10.1093/humrep/dep012

human reproduction **ORIGINAL ARTICLE** *Embryology*

A novel embryonic stem cell line derived from the common marmoset monkey (*Callithrix jacchus*) exhibiting germ cell-like characteristics

Thomas Müller[1], Gesine Fleischmann[2,4], Katja Eildermann[1], Kerstin Mätz-Rensing[3], Peter A. Horn[4], Erika Sasaki[5], and Rüdiger Behr[1,6]

[1]Stem Cell Research Group, German Primate Center, Kellnerweg 4, 37077 Göttingen, Germany [2]Institute for Transfusion Medicine, Hannover Medical School, 30625 Hannover, Germany [3]Department of Infectious Pathology, German Primate Center, Kellnerweg 4, 37077 Göttingen, Germany [4]Institute for Transfusion Medicine, University Hospital Essen, Germany [5]Laboratory of Applied Developmental Biology, Marmoset Research Department, Central Institute for Experimental Animals, Kawasaki, Japan

[6]Correspondence address. Tel: +49-551-3851-132; Fax: +49-551-3851-288; E-mail: rbehr@dpz.eu

BACKGROUND: Embryonic stem cells (ESC) hold great promise for the treatment of degenerative diseases. However, before clinical application of ESC in cell replacement therapy can be achieved, the safety and feasibility must be extensively tested in animal models. The common marmoset monkey (*Callithrix jacchus*) is a useful preclinical non-human primate model due to its physiological similarities to human. Yet, few marmoset ESC lines exist and differences in their developmental potential remain unclear.

METHODS: Blastocysts were collected and immunosurgery was performed. cjes001 cells were tested for euploidy by karyotyping. The presence of markers for pluripotency was confirmed by immunofluorescence staining and RT–PCR. Histology of teratoma, *in vitro* differentiation and embryoid body formation revealed the differentiation potential.

RESULTS: cjes001 cells displayed a normal 46,XX karyotype. Alkaline phosphatase activity, expression of telomerase and the transcription factors OCT4, NANOG and SOX2 as well as the presence of stage-specific embryonic antigen (SSEA)-3, SSEA-4, tumor rejection antigens (TRA)-1-60, and TRA-1-81 indicated pluripotency. Teratoma formation assay displayed derivatives of all three embryonic germ layers. Upon non-directed differentiation, the cells expressed the germ cell markers *VASA*, *BOULE*, *germ cell nuclear factor* and *synaptonemal complex protein 3* and showed co-localization of VASA protein within individual cells with the germ line stem cell markers CD9, CD49f, SSEA-4 and protein gene product 9.5, respectively.

CONCLUSIONS: The cjes001 cells represent a new pluripotent ESC line with evidence for enhanced spontaneous differentiation potential into germ cells. This cjes001 line will be very valuable for comparative studies on primate ESC biology.

Key words: embryonic stem cell / common marmoset / germ cell / non-human primate / pluripotency

Introduction

Cell replacement therapy using pluripotent or multipotent stem cells holds great promise for regenerative treatment of a vast number of degenerative diseases. However, it is still disputed if embryonic stem cells (ESC), somatic stem cells or recently described induced pluripotent stem (iPS) cells are best suited for cell replacement studies in preclinical and possible future clinical applications (Meissner *et al.*, 2007; Okita *et al.*, 2007; Wernig *et al.*, 2007; Yu and Silva, 2008). This open issue needs extensive further investigation with all cell types being considered as sources for cell replacement therapies. Therefore, the safety and potential of all respective cell types have to be tested in preclinically relevant animal models.

Mouse ESC differ from non-human primate and human ESC cells with respect to cell culture requirements, morphology, physiology and gene expression, reflecting significant differences between mouse and primate embryogenesis and physiology (Fougerousse *et al.*, 2000; Ginis *et al.*, 2004; Turnpenny *et al.*, 2006). Therefore, it is of fundamental importance to study primate ESC. But beside ethical concerns as well as legal limitations in several countries using

human ESC, further doubts are related to the clinical safety of the potential therapies using pluripotent stem cells (Stojkovic et al., 2004). It has to be ensured that transplanted cells are not tumorigenic and that cell replacement therapy does not cause other harmful long-term side effects. Furthermore, a real benefit from cell replacement therapy has to be demonstrated for the treated individual in preclinical studies. Since primates and mice differ significantly and several neurological diseases, such as Parkinson's or Alzheimer's disease, cannot be properly mimicked, especially with regard to their cognitive deficits, non-human primate models are of great relevance. To provide the best preclinical test systems, non-human primate disease models are needed in combination with allogenic replacement cells. This ensures that all cell–cell and cell–matrix interactions as well as all ligand–receptor interactions probably needed during cell replacement therapy properly function in the respective preclinical non-human primate disease model. Hence, although previous results from mouse ESC have provided invaluable insight in stem cell biology, the potential of clinical stem cell applications in humans must be pioneered in non-human primate species (Wolf et al., 2004) such as macaques and marmoset monkeys.

The common marmoset monkey (*Callithrix jacchus*) is readily available as a non-human primate model that exhibits many physiological similarities to humans (Michel and Mahouy, 1990; Mansfield, 2003; Zuhlke and Weinbauer, 2003; Eslamboli, 2005). However, only a few ESC lines of this species exist to date. More than 10 years ago Thomson et al. (1996) created eight ESC lines from the common marmoset, but these lines are no longer available (J. Thomson, personal communication). We recently continued research with marmoset ESC by creating and characterizing the three lines: CMESC20, CMESC40 and CMESC52 (Sasaki et al., 2005). Nevertheless, the more ESC lines from one species that are available the better, and the more profound the knowledge about a certain stem cell type from a certain species will be. For instance, human and non-human primate ESC lines diverge in their karyotype, gene expression and differentiation potential (Heins et al., 2004; Chen et al., 2008). To have available a broad collection of ESC lines, isolated from embryos at different developmental stages and sex, will benefit research on the spectrum of intra- and inter-cell line-specific varieties and epigenetic stability.

In this article, we established and characterized a fourth marmoset ESC line (cjes001) that could be cultivated successfully for over 24 months (passage 84). Besides the potential to develop into somatic cell types, this cell line also revealed strong potential to develop into germ cells upon spontaneous differentiation.

Materials and Methods

Recovery of blastocysts and initial culture

All procedures were carried out according to German and Japanese Animal Experimentation Law and all animal experiments in Japan were approved by the institutional animal care and use committee, and were performed in accordance with institutional guidelines. Animals were housed according to standard German and Japanese Primate Centre practice for the common marmoset. The method of blastocyst recovery has been described in detail (Sasaki et al., 2005). Briefly, marmoset preimplantation embryos were recovered from adult marmosets kept in the marmoset colony at the Central Institute for Experimental Animals (Kawasaki, Japan) 8 days after putative ovulation (10.7 ± 1.3 days after prostaglandin F2α administration) by uterus-flush. Out of eight animal flushes, 15 embryos were collected and immunosurgically treated to receive 15 inner cell mass (ICMs) for further cultivation. Of these 15 ICMs, 3 could be expanded until passage 10. Two of these initial lines differentiated eventually, so that finally only the cjes001 line was established. The ratio from blastocyst to established non-human-primate embryonic cell line was in this case 15:1. cjes001 cells showed flat, packed and tight colony morphology and a high nucleus to cytoplasm ratio, corresponding to the morphology reported for other primate ESC, including humans, rhesus and cynomolgus monkeys. cjes001 cells were cultured as described (Sasaki et al., 2005).

Immunosurgery and maintenance of ESC

The immunosurgery, isolation and culture of ESC lines were performed as described in detail (Sasaki et al., 2005). The zona pellucida of the marmoset blastocyst was removed by digestion in 0.1% pronase in phosphate-buffered saline (PBS). To remove the trophoblast, the blastocysts were first incubated for 45 min at 37°C in 5% CO_2 with a 10-fold dilution of anti-marmoset fibroblast rabbit serum in Dulbecco's modified Eagle's medium (DMEM). After three washes with DMEM, the blastocysts were incubated with a 5-fold dilution of guinea pig complement (Invitrogen) in DMEM for 30 min at 37°C in 5% CO_2. After mechanical removal of the trophoblast by pipetting, the ICM was plated on 3500-rad γ-irradiated mouse embryonic fibroblast (MEF) feeder cells. First passaging of the ICMs was performed after 10–14 days by physical removal of the ICM outgrowth and dissociation by vigorously pipetting. The medium used in initial ESC culture contained 80% Knockout DMEM (Invitrogen) supplemented with 20% Knockout Serum Replacement (KSR; Invitrogen), 1 mM L-glutamine, 0.1 mM MEM non-essential amino acids, 0.1 mM β-mercaptoethanol (Sigma), 100 IU/ml penicillin, 100 μg/ml streptomycin sulfate, 250 ng/ml amphotericin B and 10 ng/ml leukemia inhibitory factor. Established cell lines were cultured without amphotericin B and leukemia inhibitory factor. For passaging, ESC colonies were treated with trypsin–EDTA (0.25% trypsin, 1 mM $CaCl_2$, 20% KSR in DMEM) to remove them from feeder layer, mechanically dissociated into clumps of 10–50 cells and replated on a new irradiated MEF feeder layer. To date, the ESC line cjes001 line has been maintained under these culture conditions for 24 months (passage 84).

Immunofluorescence staining

The cjes001 colonies were grown on γ-irradiated MEF cells in foil-bottom 24-well plates (Lumox™, Greiner Bio-One, Stuttgart, Germany) for 2–5 days, fixed for 30 min in 4% paraformaldehyde, 0.04% Triton X-100 and then washed twice in PBS. The staining with primary antibodies was done according to the manufacturer's recommendations. Antibodies were diluted in Tris-buffered saline supplemented with 5% bovine serum albumin. A complete list of all primary and secondary antibodies used in this study is provided in Table 1. After 16 h incubation in first antibody dilution at 4°C, cells were washed twice in PBS, incubated for another 60 min with the respective secondary antibody covalently linked to Alexa dye A488 or A568, or the streptavidin–fluorescein isothiocyanate conjugate (STAR2B). Immunofluorescent double-stainings were performed by simultaneous incubation with both primary and secondary antibodies. Images were taken on a Zeiss Axio Observer Z1 microscope. Counterstaining reagents were propidium iodine (1:10 000, 5 min) or Hoechst 33258 (Sigma-Aldrich).

Alkaline phosphatase staining

For alkaline phosphatase staining, the alkaline phosphatase staining kit (Dako Universal LSAB Kit, K0674 AP) was used according to the

Table I Antibodies used in the study to develop a novel embryonic stem cell line from the common marmoset monkey

Antibodies	Host	Company	Cat-No.
Anti-DDX4/MVH/VASA	Rabbit	Abcam	Ab 13840-100
Anti-VASA	Goat	R&D Systems	AF2030
Anti-CD49f (Biotin)	Rat	Biozol	313604
Anti-CD9 (Biotin)	Mouse	Serotec	MCA469B
Anti-PGP9.5	Rabbit	DAKOcytomation	Z5116
Anti-human Nanog	Goat	R&D Systems	AF1997
Anti-Oct3/4	Rabbit	Santa Cruz	SC-9081
Anti-Sox2	Rabbit	Chemicon	AB5603
Anti-β-Actin	Mouse	Sigma	A-1978
Anti-SSEA1	Mouse	Chemicon	MAB 4301
Anti-SSEA3	Rat	Chemicon	MAB 4303
Anti-SSEA4	Mouse	Chemicon	MAB 4304
Anti-TRA-1-60	Mouse	Chemicon	MAB 4360
Anti-TRA-1-81	Mouse	Chemicon	MAB 4381
Anti-AFP	Mouse	Sigma	A-8452
Anti-Brachyury	Goat	R&D Systems	A-F2085
Anti-β-tubulin III	Mouse	Sigma	T-8660
Alexa fluor 488 mouse	Goat	Invitrogen	A-11029
Alexa fluor 488 goat	Donkey	Molecular probes	A-11055
Alexa fluor 488 rabbit	Goat	Invitrogen	A-110034
Alexa fluor 568 mouse	Goat	Invitrogen	A-11004
Alexa fluor 568 goat	Donkey	Molecular probes	A-11057
Streptavidin-FITC		Serotec	STAR2B

PGP9.5, protein gene product 9.5; SSEA, stage-specific embryonic antigen; TRA, tumor rejection antigen; AFP, α-Fetoprotein; FITC, fluorescein isothiocyanate.

manufacturer's instructions. For histochemistry, cells were fixed with 4% paraformaldehyde for 30 s, washed twice in PBS and incubated with Fuchsin as substrate for 30 min at room temperature.

Karyotypic analysis

Confluent ESC colonies were incubated for 4 h in ESC medium containing 0.02 μg/ml Colcemid (Invitrogen GmbH, Karlsruhe, Germany), and then washed once with PBS and trypsinized (15 min, 37°C). After detaching, the colonies were centrifuged (200g, 10 min) and the pellet was resuspended in 3 ml of prewarmed (37°C) 8 mM KCl/15 mM sodium citrate solution for 25 min at room temperature. After centrifugation (200g, 10 min), 2 ml of the KCl/sodium citrate solution was removed and 4 ml ice-cold MetOH/acetic acid (3:1) slowly added to the vial. After 5 min incubation at room temperature, the cells were pelleted again (200g, 10 min), 4.5 ml of supernatant removed, the remaining liquid carefully dropped on glass cover slips and dried overnight. For Giemsa staining [Sigma, 0.4% (w/v) in buffered methanol solution, pH 6.8], the dye was added for 2 min on the coverslip, then washed 10 times with aq. bidest and dried again. For chromosome analysis, the cells were incubated after fixation on the coverslips for 5 min in McIlvaine-buffer (pH 4.6) including 0.01 μg /ml fluorescence dye (Hoechst 33258, Sigma), then washed 10 times with aq. bidest. McIlvaine-buffer containing 5 μg/ml Quinacrine mustard (Sigma Q2876) was added for 20 min. After the second staining, the cells were washed again 10 times with aq. bidest, incubated for 5 min in McIlvaine-buffer again and embedded in mounting media (Citifluor Ltd, London, UK). The chromosome analysis was performed with a Leica CW 4000 system with a modified chromosome template based on data from Sherlock et *al.* (1996).

Telomerase detection

cjes001 telomerase activity was determined by Biomax Telomerase detection kit (Biomax Inc., Ijamsville, MD, USA) according to the manufacturer's references. Telomerase from the cell extract adds telomeric repeats onto a substrate oligonucleotide and the resultant extended product is subsequently amplified by PCR (http://www.biomax.us). Briefly, 1×10^6 cjes01 cells were lysed and the cell extract was added to a quantitative telomerase determination pre-mix in a real-time PCR reaction utilizing SYBR green for 37 cycles. As controls, MEFs, immortal green monkey kidney cells (COS7) and SYBR green, exclusive of cell extract, were used.

Reverse transcriptase–polymerase chain reaction

RNA from cjes001 or teratoma was isolated by RNeasy kit (Qiagen, Hilden, Germany) according to the manufacturer's recommendation. First-strand complementary DNA (cDNA) was synthesized with Omniscipt RT Polymerase (Qiagen) and cDNA was amplified in 35 cycles (denaturation 95°C 1 min/annealing 60°C 30 s/elongation 72°C 60 s) with 2.5 U BiothermStar *TAQ* Polymerase (Genecraft, Luedinghausen, Germany) in PCR reaction buffer [160 mM $(NH_4)2SO_4$, 670 mM Tris–HCl, pH 8.8, 15 mM $MgCl_2$, 0.1% Tween 20], 0.2 mM dNTP and 0.5 mM of each primer. cDNA from MEF cells and mock reverse transcription without RT provided negative controls. A complete list of oligonucleotides used in this study is shown in Table II. If marmoset DNA sequences were unavailable, the expected sizes of the PCR products were deduced from alignments of the homologous human and mouse sequences. Selected RT–PCR products were verified by DNA sequencing (data not shown). Normal monkey tissues exhibiting considerable expression of the respective genes served as positive controls.

Embryoid body formation

To study embryoid body (EB) formation, undifferentiated ESC were removed from the MEF layer by graduated trypsination using 0.25% trypsin that was supplemented with 1 mM $CaCl_2$ and 20% KSR until the colonies detached from the feeder layer, further dissociated using 0.25% trypsin in PBS with 20% KSR and 1 mM $CaCl_2$, and cultured in hanging drop cultures for 14–20 days in DMEM (10% fetal bovine serum) with a medium change every 3 days. The EBs were frozen in OCT Compound (Tissue-Tek, Sakura Finetek Europe B.V., Zoeterwoude, The Netherlands) for cryosections, prepared for semi-thin sections according to previously published protocols (Godmann et *al.*, 2008) or used in parallel for RT–PCR.

In vivo differentiation analysis and histology of teratoma

Eight weeks after subcutaneous injection of $1–3 \times 10^6$ cjes001 cells, tumor formation could be observed in non-obese diabetic/severely compromised immunodeficient (NOD/SCID) mice. The tumors were resected from the mice, fixed in Bouin's fixative (0.9% picric acid, 9.6% formaldehyde and 4.8% acetic acid) for 5 h, further treated according to standard histological protocols for paraffin-embedded tissues and sectioned at 5 μm for hematoxylin and eosin staining. Parts of the tumor were snap-frozen in liquid nitrogen for RNA analysis. RT–PCR analysis was performed as described above. As a positive control for teratoma formation,

Table II Primers used and their respective PCR fragment sizes

Name	Primer	Annealing temperature (°C)	Expected PCR product (bp)
AFP	5′-CAGAAAYACATCSAGGAG AG-3′ 5′-GAGCTTGGCACAGATCCTTG-3′	58	390
BexRex	5′-ACA GGC AAG GAT GAG AGA AG-3′ 5′-CCC ACG TAA ACA AGT GAC AG-3′	60	269
Boule	5′-GCGACGCAAACATCAAACCAG-3′ 5′-GAACACATCCACCATCCTGTG-3′	58	187
Brachyury	5′-CTGCYTAYCAGAAYGAGGAGA-3′ 5′-GGTTGGAGARTTGTTCCGATG-3′	58	299
CD34	5′-AGCCT-GTCACCTGGAAATGC-3′ 5′-CGTGTTGTCTTGCT-GAATGGC-3′	60	627
DAZL	5′-CCAGTCCTCATCAGCTGCAAC-3′ 5′-CAACATAGCTCCTTTGCTCCC-3′	58	306
FoxD3	5′-CGACGAC-GGGCTGGAGGAGAA-3′ 5′-ATGAGCGCGATGTAC-GAGTA-3′	60	356
GCNF (hs)	5′-GGT GAT AGT GAC CAC AGT TCC-3′ 5′-CTG CTT GCT GTA AAC GGT GAG-3′	60	501
Nanog	5′-A A ACAGAAGACCAGAACTGTG-3′ 5′-AGTTGTTTTTCTGCCACCTCT-3′	60	190
Nestin	5′-GCCCTGACCACTCCAGTTTA-3′ 5′-GGAGTCCTGGATTTCCTTCC-3′	60	200
Oct3/4	5′-CCTGGGGGTTCTATTTGGGA-3′ 5′-TTTGAATGCATGGGAGAGCC-3′	60	530
SCP3 (hs)	5′-CAG GAA ATC TGG GAA GCC GTC-3′ 5′-CTT CCG AAC ACT TGC TAT CTC-3′	60	660
Sox2	5′-AGAACCCCAAGATGCACAAC-3′ 5′-GGGCAGCGTGTACTTATCCT-3′	60	200
β-Actin	5′-CATG GAGAAGATCTG GCACCAC-3′ 5′-GATCTCCTTCTGCATCCTGTC-3′	58	689
βIII tubulin	5′-CATGTCCATGAAGGAGGTGGA-3′ 5′-GTGAACTCCATCTCATCCATG-3′	58	260
Vasa	5′-TTG GGA CTT GTG TAA GAG CTG-3′ 5′-CCC GAT CAC CAT GAA TAC TTG-3′	58	554

DAZL, deleted in azoospermia-like; GCNF, germ cell nuclear factor; SCP3, synaptonemal complex protein 3.

murine ESC were utilized, whereas PBS was injected for the negative control.

In vitro differentiation

To spontaneously differentiate the cjes001 cells, the colonies were removed from the MEF layer by trypsinization, dissociated using 0.25% trypsin in PBS with 20% KSR and 1 mM $CaCl_2$, and cultured on gelatin-coated petri dishes (Nunc) in MEF-medium. After 7–10 days, the cells had lost their characteristic undifferentiated morphology and were collected for RT–PCR or analyzed by immunofluorescence staining as described above.

Western blot analysis

Western blot analysis was performed as described (Quintana *et al.*, 1993). Briefly, about 50 mg of testis tissue or stem cell culture material was mechanically homogenized (3 × 30 s) in 2.5 ml IMP buffer [0.15 M NaCl, 20 mM HEPES, 1 mM EDTA and a protease inhibitor cocktail 1:10 (Sigma #P8340), at pH 7.4] using a tissue homogenizer, centrifuged (10 min, 750 g, 4°C) and resuspended in 2.5 ml lysis buffer (IMP buffer + 0.5% Nonidet P40). The protein content was determined by BCA protein assay kit (Novagen #71285-3) and equal amounts of protein per lane were loaded onto a sodium dodecyl sulfate gel. A protein marker (Novex sharp prestained protein standard, Invitrogen) served as size standard. After electrophoresis, the gel content was transferred to a polyvinylidene difluoride membrane (Amersham Hybond-P) in an electrophoresis chamber (Roth, 100 V, 1.2 h, 300 mA). The membrane was washed in PBS, incubated for 1 h in blocking solution and stained with the primary antibody (1:500) overnight (4°C). After 3 × 5 min washes in PBS, the secondary, horse-radish peroxidase conjugated antibody (1:10 000) was added for 1 h and again washed 2 × 15 min. The detection was carried out with an enhanced chemiluminescence kit (Amersham #RPN2209) in an Ecomaxx X-ray Film developer.

Results

cjes001 shows typical ESC morphology and a normal karyotype

Out of 15 ICM initially cultured, the cjes001 line was established. This line conserved its typical ESC morphology (Fig. 1A and see Sasaki

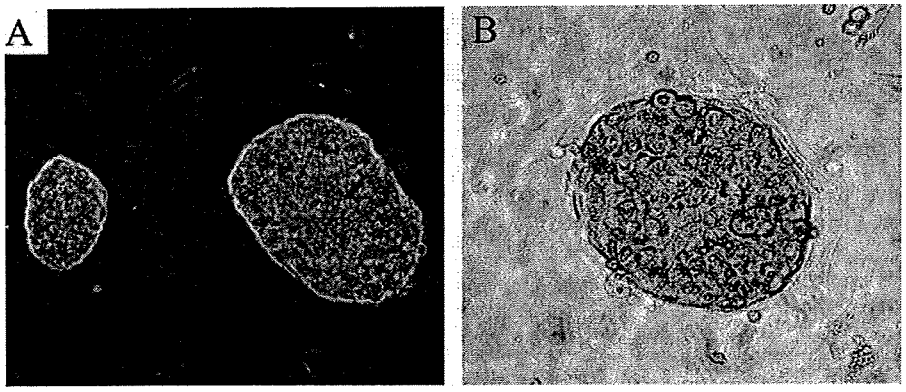

Figure 1 (**A**) Light microscopy shows tightly packed cell colonies with distinct boundaries. (**B**) Positive staining for alkaline phosphatase.

et al., 2005) and marker expression for 24 months (84 passages) and remained positive for alkaline phosphatase (Fig. 1B). The doubling time of cjes001 monitored by 5-bromo-2-deoxyuridine was roughly 19 h (data not shown). Karyotyping analysis after 64 passages showed a regular 46, XX chromosome set (Fig. 2).

cjes001 cells express undifferentiated ESC marker molecules

Immunofluorescence staining revealed the expression of the transcription factors OCT4, NANOG and SOX2 (Fig. 3), which serve as markers for pluripotency of undifferentiated ESC (Boyer *et al.*, 2005). All factors localized to the nucleus. Upon spontaneous differentiation of marmoset ESC, the expression of the pluripotency markers OCT4 and NANOG is greatly diminished at the mRNA level but not completely abolished, whereas SOX2 could not be detected in differentiated cells by RT–PCR (Fig. 4). The pluripotent cell surface antigens (Lanctot *et al.*, 2007) stage-specific embryonic antigen (SSEA)-3 and SSEA-4 (Fig. 5A–I) and keratan sulfate (tumor rejection) antigens TRA-1-60 and TRA-1-81 (Fig. 6A–F) were also strongly expressed by undifferentiated ESC. Quantitative real-time PCR analysis showed high levels of telomerase activity. The detected activities were 5-fold higher than in highly proliferative MEFs and approximately twice as high as in the SV40 virus-mediated immortalized monkey control cell line COS7 (Fig. 7).

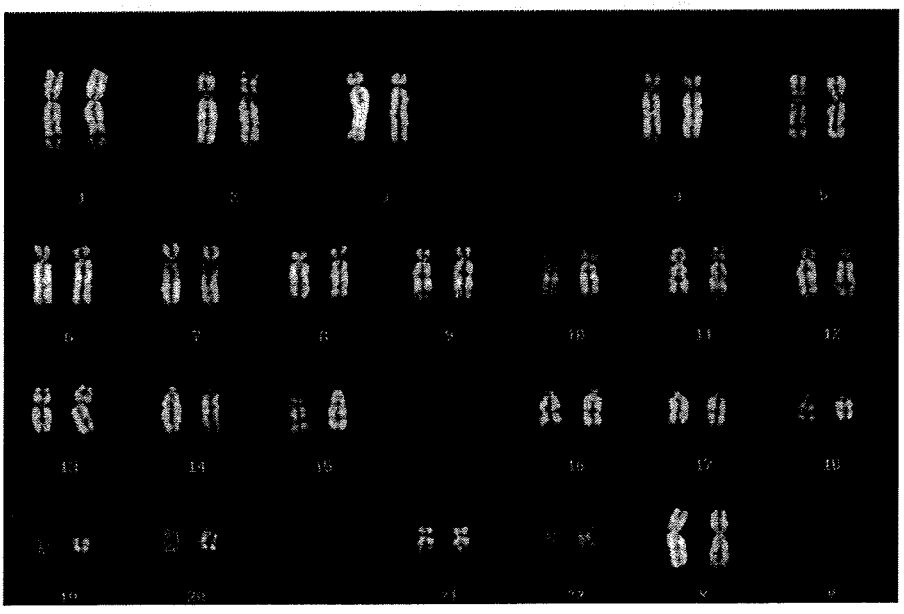

Figure 2 cjes001 cells exhibit a normal 46, XX karyotype after 64 passages.